MASTERARBEIT | MASTER'S THESIS

Titel | Title

Characterization of immune factors involved in the regulation of intestinal stem cell homeostasis

verfasst von | submitted by

Hannah Maria Sträußnigg BSc

angestrebter akademischer Grad | in partial fulfilment of the requirements for the degree of

Master of Science (MSc)

Wien | Vienna, 2024

Studienkennzahl lt. Studienblatt | Degree programme code as it appears on the student record sheet:	UA 066 834
Studienrichtung lt. Studienblatt | Degree programme as it appears on the student record sheet:	Masterstudium Molekulare Biologie
Betreut von | Supervisor:	Univ.-Prof. David Berry Privatdoz. PhD

I. Acknowledgments

First and foremost, I would like to thank my supervisors Dr. Sjoerd van der Post and Prof. David Berry for their persistent support and guidance throughout this project and for introducing the world of science to me with great enthusiasm. Their expertise and advice were invaluable for my path to becoming a scientist.

Next, I want to thank Dr. Iwona Myszor for her help and inspirational comments. I would also like to express my gratitude to Dr. Brendan Dolan for his advice and help, I appreciated it very much.

Furthermore, I want to thank all members of the Mucin Biology Groups at the University of Gothenburg for creating a welcoming and inspirational workspace. I am especially grateful for my fellow colleague Rebecka Simre, who made me look forward to work every day.

Moreover, I want to send special thanks to my family for their emotional support, their continuous encouragement and for being with me throughout this exciting journey.

Lastly, I want to thank my friends, both Austrian and Swedish, for making me feel at home wherever I go.

II. List of contents

III. Abstract

The regenerative potential of the intestinal epithelium is established by rapidly cycling intestinal stem cells (ISCs), residing at the base of the crypt. Cytokines, secreted from gut-resident innate and adaptive immune cells, play a crucial role in maintaining the delicate balance of ISC renewal and differentiation. A large body of evidence points towards the involvement of these cytokines in the production of reactive oxygen species (ROS), both in a physiological as well as in a pathological context. Recently, it has been shown that ROS generation in the colon is mainly driven by NADPH oxidase 1 (NOX1), which promotes the proliferation of colonic stem cells. In this study, we aimed to elucidate the role of selected cytokines on ISC function and development, with the goal of establishing a link between stem cell proliferation and NOX1-mediated ROS production. Moreover, we investigated the capacity of NGS Wnt-Fc, a Wnt3a surrogate, to support ISC maintenance and aimed to establish a NGS Wnt-Fc-expressing cell line in order to optimize organoid culture conditions. For the first part of the project, we tested a library of cytokines on colonic organoid cultures established from mouse models and assessed their effects on proliferation and differentiation using microscopy, fluorescence- and luminescence-based plate-reader assays and mass spectrometry. For the second part, we created a mutated NGS Wnt-Fc version using DNA cloning techniques and studied protein production upon transient and stable transfection into HEK293T cells. Our results have identified interleukin-13 (IL-13) and interleukin-22 (IL-22) as potent drivers of goblet cell differentiation, with IL-13 demonstrating differentiation-promoting effects even in the presence of stem cell-maintaining cues. Furthermore, we describe interleukin-17A (IL-17A) as a strong promoter of NOX1-mediated ROS generation in the colon with ambiguous effects on proliferation. Lastly, we show that NGS Wnt-Fc reliably sustained organoid growth and that protein production was increased upon transient transfection with an optimized plasmid. However, further efforts are required in order to generate stable protein expression of NGS Wnt-Fc in HEK293T cells.

IV. Zusammenfassung

Das Regenerationspotenzial des Darmepithels wird durch sich schnell teilende Darm-Stammzellen (ISCs) an der Basis der Krypte etabliert. Zytokine, die von angeborenen und adaptiven Immunzellen des Darms ausgeschüttet werden, spielen eine wichtige Rolle in der Aufrechterhaltung des empfindlichen Gleichgewichts zwischen der Regeneration und Differenzierung von ISCs. Viele Studien deuten darauf hin, dass Zytokine an der Produktion reaktiver Sauerstoffspezies (ROS) beteiligt sind, sowohl im physiologischen als auch im pathologischen Kontext. Kürzlich wurde gezeigt, dass die Bildung von ROS im Colon hauptsächlich durch die NADPH-Oxidase 1 (NOX1), welche die Proliferation von Colon-Stammzellen antreibt, gefördert wird. In dieser Arbeit wurde die Rolle ausgewählter Zytokine in der Funktion und Entwicklung von ISCs untersucht, um eine Verbindung zwischen der Proliferation von Stammzellen und der NOX1-vermittelten ROS-Produktion herzustellen. Darüber hinaus wurde die Fähigkeit des Wnt3a-Surrogats NGS Wnt-Fc untersucht, die Kultivierung von ISCs zu ermöglichen, mit dem Ziel, eine NGS Wnt-Fc-exprimierende Zelllinie zu etablieren, um somit die Kultivierung von Organoiden zu optimieren. Im ersten Teil des Projekts wurde die Auswirkung einer Auswahl von Zytokinen auf aus Mausmodellen etablierte Organoid-Kulturen getestet und ihr Effekt auf Proliferation und Differenzierung mithilfe von Mikroskopie, Fluoreszenz- und Lumineszenz-basierten Plate-Reader-Assays und Massenspektrometrie ausgewertet. Im zweiten Teil der Studie wurde unter Verwendung von DNA-Klonierungstechniken eine mutierte NGS Wnt-Fc-Version hergestellt und die Proteinproduktion in HEK293T-Zellen nach transienter und stabiler Transfektion analysiert. Unsere Ergebnisse zeigen, dass Interleukin-13 (IL-13) und Interleukin-22 (IL-22) die Differenzierung von Becherzellen maßgeblich fördern, wobei IL-13 selbst in Gegenwart stammzellenerhaltender Faktoren differenzierungsfördernde Effekte aufweist. Darüber hinaus identifizierten wir Interleukin-17A (IL-17A) als starken Förderer der NOX1-vermittelten Bildung von ROS im Colon, mit uneindeutigen Auswirkungen auf die Zellproliferation. Letztendlich wird gezeigt, dass NGS Wnt-Fc die Kultivierung von Organoiden unterstützt und dass die Proteinproduktion nach transienter Transfektion mit einem optimierten Plasmid erhöht wurde. Weitere Untersuchungen sind jedoch erforderlich, um eine stabile Expression von NGS Wnt-Fc in HEK293T-Zellen zu erreichen.

1. Introduction

1.1. The intestinal epithelium

The mammalian gastrointestinal (GI) tract is lined with a single layer of specialized epithelium that enables the selective uptake of nutrients, while at the same time acting as a protective barrier against luminal pathogens (Van Der Flier & Clevers, 2009) (Beumer & Clevers, 2021). With a turnover rate of 4-5 days, it is the most rapidly self-renewing tissue in adult mammals (Sato et al., 2009) (Van Der Flier & Clevers, 2009). The intestinal epithelium and the underlying lamina propria, comprising immune, vascular and structural components, together form the intestinal mucosa (Pérez et al., 2017). Structurally, the epithelial layer is arranged into a crypt-villus structure. Crypts are epithelial invaginations harboring vigorously self-renewing intestinal stem cells that confer the crypts their proliferative potential. Stem cells divide to form transit-amplifying cells that further develop into one of the terminally differentiated intestinal cell types covering the villi, which are finger-like protrusions into the gut lumen that maximize the epithelium's absorptive potential. The villus length decreases along the intestinal tract, from being highest in the duodenum, to being absent in the flat epithelium of the colon (Gehart & Clevers, 2019). Underneath the villi extend capillaries and lymph vessels which further distribute the absorbed nutrients throughout the body (Clevers, 2013).

1.2. Intestinal stem cells and their niche

Intestinal stem cells (ISCs) were initially identified as slender cells interspersed between Paneth cells at the crypt bottom in the small intestine, termed "crypt-base columnar cells" (CBCs) (Cheng & Leblond, 1974). Using lineage-tracing experiments, Cheng & Leblond (1974) showed that these CBCs were able to transfer radioactive labels to the four differentiated cell types of the intestine. Chemical mutagenesis further elucidated that this transfer pattern occurred from the crypt to the villus, giving rise to long-lived and short-lived clones respectively (Bjerknes & Cheng, 1999). The identification of Leucine-rich-repeat-containing G-protein-coupled receptor 5 (*Lgr5*$^{+}$), a target gene of the Wnt signaling pathway, as a CBC-specific marker and genetic lineage tracing in *Lgr5*$^{+}$-knock-in mice finally established *Lgr5*$^{+}$ CBCs as the stem cells of the small intestine and the colon (Barker et al., 2007). As shown by Sato et al. (2009), single *Lgr5*$^{+}$ CBCs can be isolated from intestinal crypts and expanded indefinitely in culture, giving rise to 3D-structures referred to as organoids or "mini-guts" (Beumer & Clevers, 2021).

The cellular identity of intestinal stem cells is supported by the niche they reside in at the crypt bottom and competition for niche space ensures stringent control over the ISC number (Beumer & Clevers, 2021). The ISC niche is composed of mesenchymal as well as epithelial components. The mesenchymal niche, e.g. fibroblasts, provides growth factors required for

the maintenance of ISC function (Hou et al., 2021). Furthermore, Paneth cells at the crypt bottom of the small intestine also provide extrinsic signals including niche factors, which comprise ligands of classical signaling pathways (***Chapter 1.4***), including Wnt, R-spondin, Epidermal Growth Factor (EGF) and noggin. In the colon, where Paneth cells are absent, the regenerative capacity is provided by the stroma and partly by deep secretory cells (DSCs), which are specialized cells sharing properties of Paneth cells and goblet cells, while displaying a unique secretory profile whose function is not fully elucidated (Beumer & Clevers, 2021) (McCarthy & Keely, 2023).

1.3. Differentiated cell types of the intestinal epithelium

The six different cell lineages constituting the differentiated cell types of the intestine can be broadly sub-categorized into absorptive and secretory lineages (***Figure 1***). Nutrient- and water-absorbing enterocytes make up the highest percentage (80-90 %) of differentiated cells and contain surface-enlarging microvilli, which expand the apical surface of the epithelium, thereby maximizing its absorptive capacity. Equivalently, the absorptive cells of the colon are termed colonocytes. The secretory lineage of the intestine comprises goblet cells, Paneth cells, enteroendocrine cells and tuft cells. Goblet cells play a central part in epithelial protection by secreting mucus, which acts as a lubricant and protects the epithelial surface from direct interaction with the intestinal microbiota. Furthermore, the secreted mucus serves as a shield against chemical damage and shear stress and enables gut contents to be properly expelled (Beumer & Clevers, 2021). The distribution of goblet cells in the intestinal tract follows a gradient, increasing from the duodenum to the descending colon (Van Der Flier & Clevers, 2009). Paneth cells are only found at the crypt bottom of the small intestine, and not in the colon. Besides their role in providing ISC niche factors, they play an important part in host defense by producing antimicrobial peptides, which prevent the growth of bacteria in the crypt. Another specialized cell type are chemosensory tuft cells, which aid in the mediation of immune responses under harmful conditions, including hypoxia and infection. Furthermore, microfold cells play a role in the gut's immune response by sampling intestinal components and transporting them to underlying immune cells. Finally, enteroendocrine cells produce hormones in response to specific stimuli, controlling multiple regulatory processes (Beumer & Clevers, 2021).

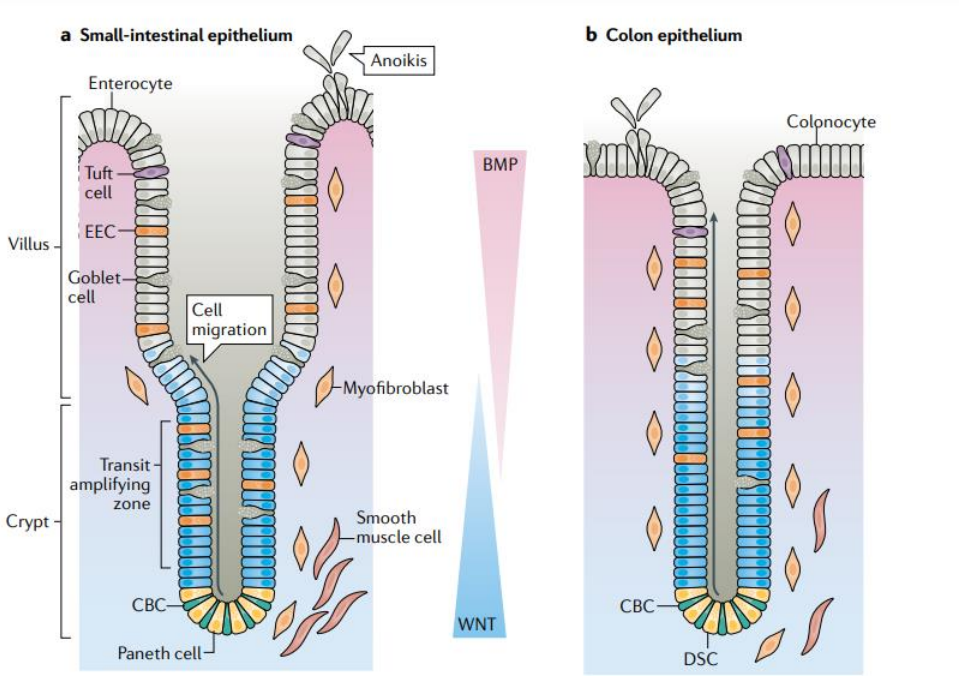

Figure 1 Crypt-villus architecture of the intestinal epithelium. a) The crypt bottom of the small intestine harbors CBCs and Paneth cells. CBCs differentiate into transit-amplifying cells and further into one of the terminally differentiated intestinal cell types (enterocytes, goblet cells, Paneth cells, tuft cells, microfold cells, enteroendocrine cells (EECs)), migrating from the intestinal crypt towards the villus. After 3-5 days, they are shed into the lumen and undergo programmed cell death (anoikis). Stem cell maintenance and differentiation are controlled by a gradient of signaling molecules obtained from the surrounding stroma (myofibroblasts, smooth muscle cells) and from Paneth cells. The highest activity of Wnt signaling is found at the crypt bottom, the highest bone morphogenetic protein (BMP) signaling at the villus tip. **b)** The colon has a flat surface and contains deep secretory cells (DSCs) instead of Paneth cells. The absorptive cells of the colon are called colonocytes (Beumer & Clevers, 2021).

1.4. Pathways involved in intestinal physiology

The delicate balance between self-renewal and lineage-commitment of CBCs is established by the activation or inhibition of classical signaling pathways. The signals controlling stem cell fate follow a spatial gradient along the crypt-villus axis (***Figure 3***) Wnt, R-spondin, Notch and EGF signaling are highest at the crypt bottom and their activity decreases towards the villus tip. For BMP signaling, this effect is reversed (Qi & Chen, 2015) (Beumer & Clevers, 2021).

The central driving force behind the proliferative potential of stem cells in the intestinal niche is the Wnt signaling pathway (***Figure 2***) (Van Der Flier & Clevers, 2009). Wnt ligands are lipid-modified proteins that mediate the formation of a heterodimeric complex between receptors of the Frizzled (Fzd) family and their co-receptors low-density lipoprotein receptor-related protein 5/6 (LRP5/LRP6) (Beumer & Clevers, 2021). In the absence of Wnt ligands, the intracellular protein β-catenin is targeted for degradation via phosphorylation events at its N-terminus. Upon binding of Wnt ligands to the Frz/LRP5/6 complex, phosphorylation is inhibited by the

inactivation of a degradation complex consisting of the tumour suppressor axin, adenomatous polyposis coli (APC) and the kinases glycogen synthase kinase 3β (GSK3) and casein kinase I (CKI). This results in the cytoplasmic accumulation of β-catenin and its subsequent translocation to the nucleus, where it replaces the inhibitor Groucho, leading to the activation of transcription factors of the T cell factor/lymphocyte enhancer factor family (TCF/LEF) involved in the activation of Wnt target genes (Van Der Flier & Clevers, 2009). In the small intestine, Wnts are produced by Paneth cells, whereas in the colon they are provided by the colonic stroma.

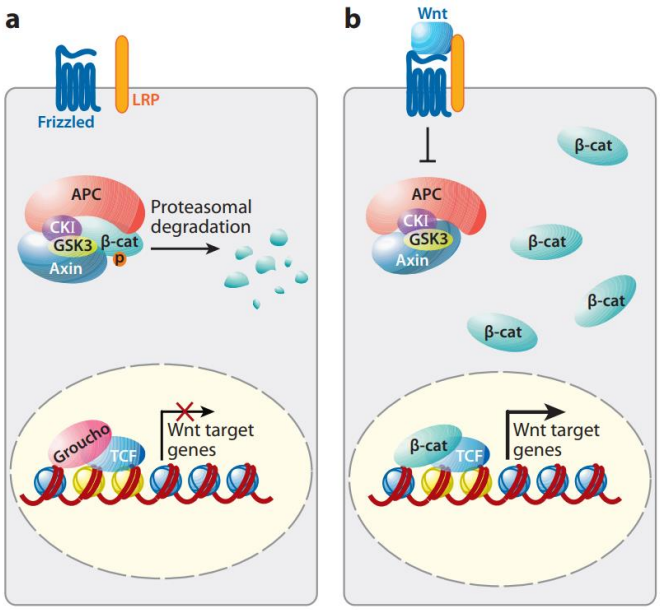

Figure 2 Wnt signaling pathway. **A)** In the absence of Wnt ligands, β-catenin is degraded by a destruction complex (APC, CKI, GSK3, Axin) and the expression of Wnt target genes is suppressed by the action of Groucho. **B)** In the presence of Wnt ligand binding, Frizzled and LRP associate and inhibit β-catenin degradation by suppression of the degradation complex, leading to its translocation into the nucleus and the induction of Wnt target genes (Van Der Flier & Clevers, 2009).

Wnt signaling is enhanced by the action of R-spondin, which acts directly through LGR5 to inhibit E3 ligase-mediated endocytosis of Fzd. Binding of the R-spondin/LGR5 complex suppresses ligase activity, thereby preventing negative-feedback mechanisms and promoting Wnt signaling.

Additionally, Notch signaling prevents differentiation by releasing the Notch intracellular domain (NCID) upon interaction of a ligand-presenting and a receptor-producing cell and subsequent activation of the Hairy and enhancer of split 1 gene (*Hes1*). This leads to the suppression of differentiation-promoting transcription factors, including AtohI. Consequently, loss of Notch signaling drives the differentiation of intestinal stem cells into secretory lineages.

Lastly, signaling via EGF is essential for maintaining stem cell proliferation. In the small intestine, EGF is produced by Paneth cells and acts via its receptor EGFR (ERBB1) to increase proliferation of CBCs. Inhibition of EGF signaling promotes cell cycle arrest without initiating differentiation, suggesting that the proliferative capacity of CBCs is uncoupled from their stem cell potential (Beumer & Clevers, 2021).

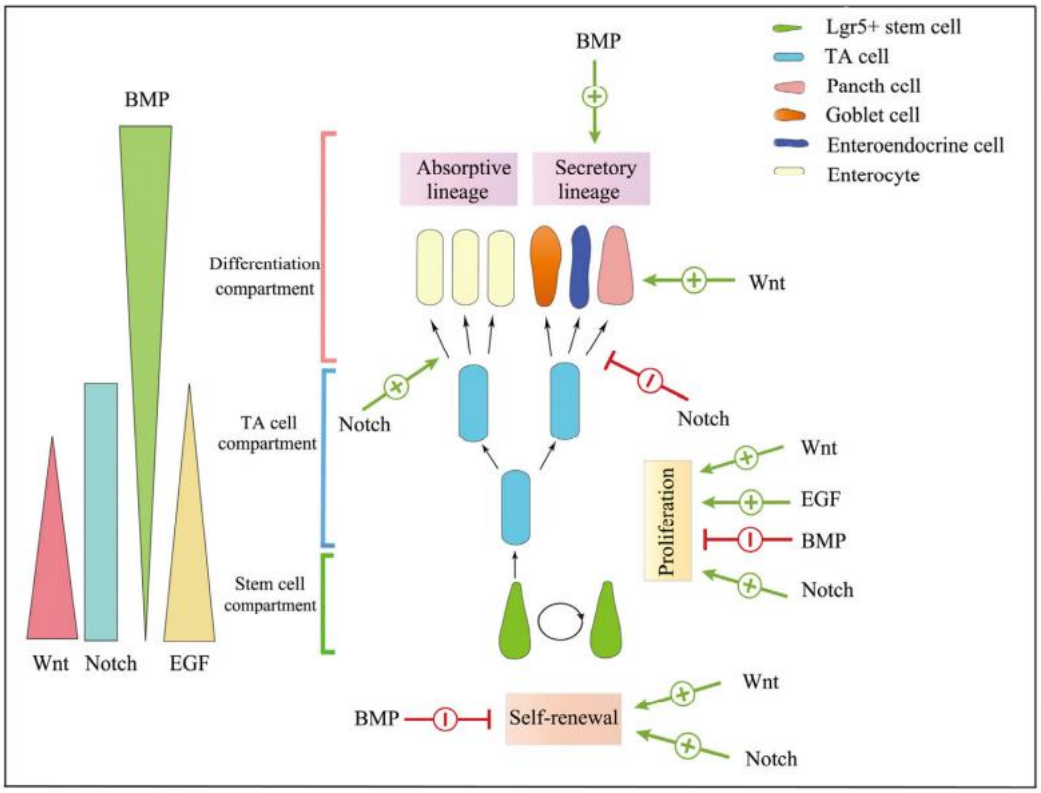

Figure 3 Signal gradients regulating stem cell fate in the intestinal compartment. Wnt, Notch, EGF and BMP signalling collectively regulate stem cell decisions along the crypt-villus axis. ISC self-renewal is promoted by Wnt and Notch activity and inhibited by BMP signalling. Furthermore, Wnt, EGF and Notch support cell proliferation. Lastly, Wnt, Notch and BMP specify differentiation events into the absorptive and secretory lineage (Qi & Chen, 2015).

In order to keep the balance between self-renewal and differentiation in intestinal stem cells, the Bone Morphogenetic Protein (BMP) pathway has to be inactivated. BMPs are produced by mesenchymal cells and show the highest concentration at the villus tip. At the crypt bottom, BMP inhibitors, including noggin, inhibit BMP signaling. BMP2 and BMP4, the primary BMPs in the gut, mediate activation of target genes via the phosphorylation of SMAD proteins upon binding to BMPR1A. BMP signaling repressing expression of stem cell genes by the recruitment of histone deacetylases via phosphorylated SMADs, thereby confining stem cells to the crypt bottom (Beumer & Clevers, 2021).

1.5. The intestinal immune system and stem cell homeostasis

The mammalian intestine constitutes the largest immune organ of the body and is exposed to a broad range of different antigens derived from commensal bacteria, dietary components and pathogens. The development and function of the intestinal immune system is strongly impacted by the gut microbiota and their metabolites. The number and frequency of immune cells differs throughout the GI tract. The lamina propria, underlying the intestinal epithelium, contains cells from the innate and the adaptive immune system, including B cells, T cells, innate lymphoid cells (ILCs), dendritic cells (DCs), macrophages, mast cells and eosinophils (Hou et al., 2021). Furthermore, immune cells constitute an important component of the stem cell niche. Besides their critical role in tissue repair, tissue-resident and circling immune cells have gained high relevance in the homeostatic regulation of intestinal stem cells (Naik et al., 2018). Specifically, cytokines secreted from mucosal immune cells regulate intestinal homeostasis, thereby playing a crucial role in the maintenance or destruction of the intestinal epithelial barrier (Neurath, 2014) (Hou et al., 2021). Under physiological conditions, the balance of pro-inflammatory and anti-inflammatory cytokines is tightly controlled to ensure the regulation of renewal and differentiation in the intestine (Biton et al., 2018). Loss of this control is implicated in the development of intestinal pathologies, such as inflammatory bowel disease (***Chapter 1.6***) (Neurath, 2014). The establishment of intestinal organoid models (***Chapter 1.8***) has allowed for great advances in the *in vitro* studies of cellular proliferation and differentiation. Furthermore, co-culturing experiments of intestinal organoids with immune cells has enabled crucial insights into the complex interplay of the intestinal epithelium and the immune system, showing an implication in gut regeneration and ISC regulation (Hou et al., 2021).

Table 1 shows the role of selected cytokines in the intestine and their implications in disease. Tumor necrosis factor α (TNF-α) is a pro-inflammatory cytokine identified as a strong driver of intestinal inflammation and displays pleiotropic effects on the different cell types of the intestine. High levels of TNF-α have been implicated with the induction of apoptosis in intestinal epithelial cells and alterations in the epithelial barrier (Friedrich et al., 2019). In IBD patients, TNF-α levels are highly increased, leading to the development of TNF-α-targeting therapies that have been shown to greatly improve the clinical picture (Neurath, 2014) . In ISCs, $CD4^+$ effector memory T cell-derived TNF-α has been shown to support ISC proliferation at low levels, whereas high levels impaired their function (Schreurs et al., 2019). T_H2-derived interleukin-13 (IL-13) is involved in inflammatory responses to induce the clearance of helminth infections by stimulating mucus production and upregulating the number of goblet cells in the intestine (Mannon & Reinisch, 2012). In ISCs, IL-13 has been shown to suppress self-renewal and to promote differentiation into tuft cells, as well as upregulating genes associated with goblet cells (Hou et al., 2021) (Lindholm et al., 2022). On a pathological level, IL-13 has been implicated with the development of ulcerative colitis (Neurath, 2014). The pro-inflammatory

cytokine interleukin-17A (IL-17A) is mainly produced by T_H17 cells and plays an important role host defense and the maintenance of intestinal integrity. The complete role of IL-17A in the intestine is complex, with mutations in IL-17A signaling being associated with the development of inflammatory bowel diseases, while the progression of colorectal cancer also appears to be favored by IL-17A signaling. In ISCs, IL-17A is associated with the differentiation into secretory cell types (Lin et al., 2022). Interferon-γ (IFN-γ), produced by T cells, ILCs and macrophages, is involved in host responses to infection and has pro-apoptotic and anti-proliferative effects in the intestine. Moreover, it has been shown to suppress the self-renewal of ISCs and is, hence, associated with a decreased ISCs number (Hou et al., 2021). Furthermore, it alters tight junction activity and promotes cell death of intestinal epithelial cells. T-cell derived interleukin-10 (IL-10) is an anti-inflammatory cytokine and has been implicated in the maintenance of intestinal homeostasis and ISC renewal, with mutations in the *IL10* gene leading to severe intestinal inflammation (Friedrich et al., 2019) (Hou et al., 2021). IL-10 suppresses the production of pro-inflammatory cytokines by antigen-presenting cells and T cells and, furthermore, induces STAT2 signaling in regulatory T cells (Neurath, 2014). Lastly, ILC-derived interleukin-22 (IL-22) has been shown to promote ISC proliferation through the activation of STAT3 signaling. Furthermore, it reduces genotoxic stress through the secretion of antimicrobial peptides and plays an essential role in mucosal wound healing (Hou et al., 2021).

Cytokine	Source in the mucosa
TNF-α	Macrophages, T cells, DCs
IL-13	ILCs, T2 cells, natural killer cells
IL17-A	T cells, ILCs
IFN-γ	T cells, ILCs
IL-10	T_{reg} cells
IL-22	T cells, DCs, ILCs

Table 1 Cytokines and their source in the mucosa (Hou et al., 2021).

1.6. Inflammatory bowel disease (IBD)

Inflammatory bowel diseases (IBDs) are chronic, relapsing pathologies of the GI tract, characterized by digestive disorders, epithelial injuries and intestinal inflammation (Saeid Seyedian et al., 2019) (Neurath, 2014). Depending on the affected region of the intestine, IBDs can be subdivided into Crohn's disease (CD) and ulcerative colitis (UC), which comprise symptoms including diarrhoea, abdominal pain and cramping, weight loss and rectal bleeding (Saeid Seyedian et al., 2019). CD can affect both the small and the large intestine, but is most common in the colon and rectum, where it manifests as discontinuous areas of inflammation. In contrast, UC occurs only in the colon and rectum in a continuous manner and affects only the mucosa, whereas CD can affect several intestinal layers (Sahoo et al., 2023).

The onset and relapse of IBDs are a complex interplay by environmental factors, microbial dysbiosis and host genetic susceptibility in combination with a compromised intestinal barrier and subsequent dysregulation of the immune response. Environmental triggers can cause alterations to the microbiome, leading to a loss of diversity and the transition to a more inflammatory state. In order for these alterations to manifest, the intestinal barrier, including the intestinal epithelium and the immune cells, needs to be impaired (Ramos & Papadakis, 2019). Mucosal immune cells respond to microbial products or antigens by secreting cytokines, promoting chronic inflammation of the gastrointestinal tract (Neurath, 2014). Under physiological conditions, the intestinal epithelium prevents the direct interaction of the microbiota on the luminal side with the underlying immune cells, keeping pro-inflammatory and anti-inflammatory immune responses tightly regulated. In IBD patients, this control is lost and the intestinal mucosa is often infiltrated with a great number of inflammatory cells, e.g. macrophages, lymphocytes and neutrophils, provoking tissue damage and sustaining the inflammatory response (Sahoo et al., 2023). Hence, elucidating the complex network of cytokine responses in healthy and diseased patients is pivotal for IBD therapy (Pavlidis et al., 2022) (Neurath, 2014). Anti-cytokine treatments as well as cytokine signaling blockers have been suggested as candidates for clinical trials, however, they display high patient-specific effects. Therefore, further research is needed to fully understand the causes of IBDs in order to be able to develop new treatment strategies.

1.7. Redox biology in the intestine

Reactive oxygen species (ROS) are a large class of oxidant molecules that are produced as a direct consequence of biological metabolism and are involved in a wide range of biological functions. They participate in reduction-oxidation (redox) reactions and can modify biological macromolecules via oxidation, thereby contributing to redox signaling and physiological processes. At physiological concentrations, ROS have mainly beneficial effects, including the killing of pathogens, wound healing and tissue repair as well as contributing to cellular signalling (Sies et al., 2022) (Sartor, 2006). However, at supraphysiological levels ROS have been implicated with cellular dysregulation, leading to a range of gastrointestinal diseases, including gastric and colorectal cancer, IBDs and celiac disease (Sies et al., 2022) (Pérez et al., 2017).

Two major sources of ROS in the intestine under physiological conditions are mitochondria and NADPH oxidases (NOXs). Mitochondria produce superoxide anion radical ($O_2^{\cdot -}$) as well as hydrogen peroxide (H_2O_2) and other oxidants via the electron transport chain. These oxidants are rapidly eliminated by antioxidants or enzymes including superoxide dismutases and peroxidases. NOXs are membrane-bound enzyme complexes that use NADPH to reduce oxygen to $O_2^{\cdot -}$ and H_2O_2 (Sies et al., 2022). In the gastrointestinal epithelium, NOXs support

self-renewal, proliferation and differentiation via the redox-dependent modulation of essential signaling pathways (Pérez et al., 2017). NADPH-oxidase 1 (NOX1) is involved in redox signaling in proliferative colonic stem cells (***Figure 4***). While the colon displays a high expression of NOX1, its activity is absent in the small intestine. NOX1 is involved in the regulation of Wnt and Notch signaling, thereby contributing to stem cell maintenance and cell fate decisions (Pérez et al., 2017). Furthermore, Van der Post et al. (2021) showed that proliferation of colonic stem cells is potentiated by the redox-dependent activation of the EGFR through NOX1-derived ROS. NOX1 activity has been shown to be altered in response to stimulation with selected cytokines, e.g. as described for TNF-α (Hsu et al., 2023).

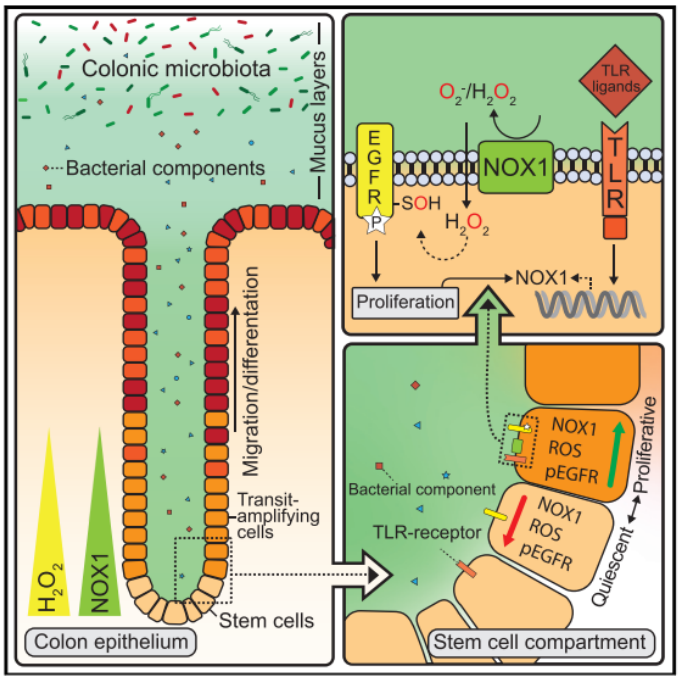

Figure 4 Schematic overview of the role of NOX1 in the colonic crypt. NOX1 is a ROS-generating enzyme, which is specifically expressed by stem cells at the base of the crypt. NOX1 activation participates in the EGFR signalling-dependent quiescent-proliferative transition responsible for epithelial renewal. NOX1-derived ROS can act as a secondary messenger via the oxidation of cysteine thiol groups (redox signalling), thereby increasing EGFR activity to maintain proliferation. NOX1 expression in colonic stem cells can be regulated via toll-like receptors allowing for the regulation of epithelial proliferation in direct response to the intestinal microbiota (Van Der Post et al., 2021).

1.8. Organoid cultivation state of the art

Organoids are stem cell-derived, self-assembling 3D models that display similar functional, structural and biological characteristics as the corresponding *in vivo* tissue. Over the last years, they have gained increasing scientific interest due to their potential applications in diagnostics, drug discovery, personalized medicine and disease modelling. Organoids pose a great advantage to immortalized cell lines, as they more accurately reflect the organ of origin and display high patient-specificity. Given the importance of the intestinal niche in the regulation of

stem cell fate, the establishment of intestinal organoids highly depends on the successful mimicry of these environmental cues (Z. Zhao et al., 2022). Sato et al. (2009) were the first to achieve long-term culture of intestinal organoids from single *Lgr5*$^{+}$ stem cells in the absence of a mesenchymal niche through the development of growth-optimized culture conditions using medium supplemented with the growth factors Wnt, EGF, noggin and R-spondin (WENR). Additionally, Matrigel, a base membrane extract containing components of the extracellular matrix as well as growth factors, was used to mimic the support provided by fibroblasts surrounding the cells in the crypt (Sato et al., 2009) (Miyoshi & Stappenbeck, 2013). In order to specifically enrich for intestinal stem cells and generate more affordable large-scale culture conditions, Miyoshi & Stappenbeck (2013) established a L-WRN supportive cell line for the production of conditioned medium. This cell line secretes Wnt3a as well as noggin and R-spondin required for stem cell propagation and is supplemented with 20% fetal bovine serum (FBS). The introduction of serum is required for the lipid-stabilization of the water-insoluble Wnt3a and, in addition, provides a source of EGF (Tüysüz et al., 2017). A major advantage of this method is the possibility to produce conditioned medium relatively easily and cost-effectively without the need of obtaining expensive stem cell factors commercially. However, a considerable drawback is that the addition of serum introduces undefined parameters into the culture conditions (Mihara et al., 2016). Furthermore, conditioned medium displays an inherent batch-to-batch variation, impacting experimental reproducibility (Zhao et al., 2022). Hence, a great number of engineering approaches to generate optimal organoid growth support have been undertaken (Janda et al., 2017). Among them is the establishment of a water-soluble Next-Generation-Wnt (NGS Wnt-Fc) variant by Miao et al. (2020). NGS Wnt-Fc is water-soluble, enabling culture in serum-free conditions, and displays high Frizzled-subtype specificity. Furthermore, NGS Wnt-Fc was demonstrated to be superior to Wnt3a-containing conditioned medium in organoid expansion and single cell organoid outgrowth (Miao et al., 2020).

1.9. Specific aims

This project was divided into two parts. The first aim of the project was to investigate the effects of a library of cytokines on ISC function and development, with the goal of identifying drivers and inhibitors of proliferation and differentiation within the context of NOX1-mediated generation of ROS. As the experimental setup, colonic organoid cultures established from different mouse models were treated with a library of candidate cytokines and the effects of treatment were assessed at defined timepoints using microscopy techniques, fluorescent and luminescent plate-reader assays as well as mass spectrometry. Based on this, we aimed to translate alterations in NOX1 expression into changes in stem cell homeostasis in order to extend our knowledge of the regulatory mechanisms in gut homeostasis within the complex interplay of ISCs and immune factors.

The second aim of this project was the establishment of a NGS Wnt-Fc-producing HEK293T cell line with the goal of optimizing organoid culture conditions. In the state of the art *in vitro* cultivation of organoids conditioned medium, containing the niche factors Wnt3a, R-spondin and noggin, is used to support organoid growth and maintenance (Miyoshi & Stappenbeck, 2013). However, serum-supplementation is required for the lipid-stabilization of the water-insoluble Wnt3a, introducing undefined parameters into the experimental setup (Tüysüz et al., 2017). The water-soluble NGS-Wnt-Fc surrogate has been shown to effectively support organoid expansion and long-term organoid cultivation and abolishes the need for serum addition. In order to generate a NGS Wnt-Fc-producing cell line, we first aimed to generate a NGS Wnt-Fc plasmid displaying increased protein production by introducing a Kozak sequence into the original plasmid. Furthermore, we assessed expression levels upon transient transfection into HEK293T cells by SDS-PAGE western blotting. Finally, we aimed to integrate the protein-coding target sequence into the HEK293T cellular genome using the PiggyBac transposon system in order to generate a stably producing NGS Wnt-Fc cell line.

2. Materials and Methods

2.1. Cell culture

2.1.1. Primary cell culture

2.1.1.1. Experimental models

Colonic stem cells were isolated from conventionally raised mice (ConvR), ConvR mice with transgenic mCherry-labelled MUC2 (redMUC2) and germ-free (GF) mice. All mice were on C57BL/6 genetic background and maintained and sacrificed under controlled regulations of the local animal ethics and handling committee.

2.1.1.2. Thawing of colonic organoids

Mouse spheroid cultures were cultivated from previously established distal colonic cell lines and stored in a -150 °C N_2 storage system. The cryovials were placed in a bead bath and warmed up to 37 °C for 2 minutes until just thawn. Then, the primary cells were transferred into a tube containing pre-warmed washing medium consisting of Advanced Dulbecco's Modified Eagle Medium/Ham's F-12 (DMEM/F12, Gibco, 12634-010) supplemented with 10 % Fetal Bovine Serum (FBS, Gibco, A52567-01), 1 % GlutaMAX (Gibco, 35050-061) and 100 U/mL Penicillin-Streptomycin (Gibco, 15140-122) and centrifuged at 200 g for 5 minutes. Subsequently, the supernatant was aspirated and the cell pellet was resuspended in washing medium, transferred to a smaller tube and again centrifuged at 200 g for 5 minutes. To prepare the cells for seeding, the tube was placed on ice for 5 minutes. Next, the cells were resuspended in basement membrane extract (BME) (Cultrex, 3433-010-01) and seeded onto a 24-well cell culture plates (Corning, #3527) at the desired density. Immediately after, the plate was placed upside down into the incubator to let the BME polymerize and prevent the cells from settling on the bottom of the plate. After 15 minutes, the cells were overlaid with 500 µL of 50% L-WRN conditioned medium (50CM) with 10 µM Y27632 (Rock inhibitor, Stem cell, 72307), obtained from a fibroblast-like cell line engineered to produce the stem cell factors Wnt3a, R-spondin and Noggin, and stored at 37 °C until passaging, as established by Miyoshi & Stappenbeck (2013).

2.1.1.3. Maintenance of intestinal organoid cultures

Mouse intestinal organoid cultures were passaged every 3-4 days. The medium was aspirated and ice-cold 1X phosphate buffered saline (PBS) with 5 mM EDTA (Invitrogen, #15575-038) was added to each well to induce dissociation of cell-cell- and cell-matrix-interactions. After this, the BME was gently scraped from the bottom of each well using a P1000 pipette tip, shortly resuspended and transferred to a tube. Then, the cell suspension was centrifuged at 300 g for 5 minutes and the supernatant was aspirated. The cell pellet was incubated in pre-warmed TrypLE Express (Gibco, #12605-028) for 1 minute at room temperature. To assist

dissociation, the pellet was slowly resuspended using a P1000 pipette, applying light pressure on the bottom of the tube. To inactivate the TrypLE, washing medium was added to the cells and the tube was centrifuged at 300 g for 5 minutes. After removing the supernatant, the tubes were put on ice for 5 minutes. The cell pellet was resuspended in ice-cold BME and the suspension was seeded onto the center of each well of a 24-well plate. Then, the plate was transferred to the incubator upside down for 5-10 minutes. Finally, the wells were overlaid with 50CM and incubated at 37 °C until the next passaging. The culture medium was changed every 2 days.

2.1.1.4. Freezing of intestinal organoids

Freezing medium (DMEM with 20 % FBS and 10 % dimethyl sulfoxide (DMSO)) was prepared for freezing down intestinal organoid cultures. The culture medium was removed and the freezing medium was added to the cells. Next, the BME was scraped off and the cell suspension was transferred to cryovials. The vials were placed into a cooling container and kept at -80 °C for 24 h. After this, they were stored in a -150 °C storage system.

2.1.1.5. *In vitro* differentiation of colonic organoids

In vitro differentiation of redMUC2 organoid cultures (ConvR) was induced by switching from 50CM to ENR medium, consisting of basal medium with DMEM/F12, 1% GlutaMAX, Penicillin-Streptomycin at 100 U/mL and 10 mM HEPES (Gibco, 15630-080) supplemented with 1X B-27 Supplement (Gibco, 17504-044), N-2 Supplement (Gibco, 17502-048), N-acetyl cysteine (1 mM), 500 ng/mL R-spondin 1 (Prepotech, 315-32), 100 ng/mL Noggin (Prepotech, 250-38) and 10 ng/mL EGF (Thermo Fisher Scientific, PMG8041). First, the cultures were grown in 50CM on black or white 96-well microplates with a clear bottom (Corning, #353219) for 48 h. Then, they were differentiated in ENR supplemented with cytokines (***Chapter 2.1.1.6***) for 72 h, after which the mCherry-signal and the cell number were determined (***Chapter 2.1.1.9***)***.***

2.1.1.6. Cytokine treatment of colonic organoid cultures

A library of selected cytokines was used to stimulate colonic organoid cultures. Cytokine stocks were prepared in PBS with 0.1 % Bovine serum albumin (BSA) and used at 10 ng/mL (TNF-α, IL-17a, IL-10, IL-22) and 20 ng/mL (IL-13, IFN-γ).

2.1.1.7. Determination of ROS production in colonic organoid cultures

To study the effect of cytokine stimulation on ROS production, colonic organoid cultures were grown on white 96-well plates in 50CM for 24 h and then stimulated with selected cytokines for 48 h. Superoxide ($O_2^{\cdot-}$) was determined based on the ROS-induced oxidation of a L-012 substrate (FUJIFILM Wako, 120-04891), a luminol-based probe that reacts with $O_2^{\cdot-}$ to emit luminescence. To induce the reaction, L-012 was diluted (1:1000) in phenol-free DMEM (Gibco, 21063029) and the luminescent signal was measured over 30 minutes at 37 °C with 5

% CO_2 using the ClarioStar platereader (BMG Labtech). ROS production was measured in combination with the CellTiter-Fluor Cell Viability Assay (***Chapter 2.1.1.8***).

2.1.1.8. Fluorescence-based determination of cell proliferation in organoid cultures

The number of viable cells in undifferentiated colonic organoid populations was determined using the CellTiter-Fluor Cell Viability Assay (Promega, G6081). To this end, the CellTiter-Fluor reagent was prepared by combining the glycyl-phenylalanyl-aminofluorocoumarin (GF-AFC) substrate with the Assay Buffer (1:200) and overlaying the wells with the required volume. The fluorescent signal emitted upon cleavage of the substrate by constitutively active live-cell proteases was determined using the ClarioStar platereader. The readout was performed in combination with the L-012 assay (***Chapter 2.1.1.7***).

2.1.1.9. Determination of cell number and goblet cell differentiation in redMUC2 organoids

The number of viable cells in differentiating organoid cultures was determined using the CellTiter-Glo Luminescent 2.0 Cell Viability Assay (Promega, G9241), correlating the quantitation of ATP present with the number of metabolically active cells. The CellTiter-Glo reagent was prepared as stated in the protocol and stored at -20 °C. To perform the readout, the reagent was thawed in the dark and combined 1:1 with PBS or Fluorobrite DMEM (Gibco, A18967-01) to determine the mCherry-signal obtained from MUC2-expressing cells. The wells were overlaid with the required volume and incubated for 15 minutes by shaking on medium intensity. To minimize background signal obtained for fluorescence, black or white sealing tapes (Revvity, NC9425162) were used to cover the bottom of black or white 96-well microplates respectively.

2.1.1.10. Cytotoxicity assay

Cytotoxicity was determined using the LDH-Glo Cytotoxicity Assay (Promega, J2380). The assay determines the number of dead cells based on the content of lactate dehydrogenase (LDH) present in the cell culture medium, which is released upon disruption of the cell membrane. The reaction components were prepared and stored according to the user manual. As the experimental setup, organoids were cultured on white 96-well plates and treated with cytokines for 48 h. To perform the readout, a defined volume was taken from each triplicate and added to LDH storage buffer. Next, the diluted samples were pipetted onto a 96-well plate and LDH detection agent was added (1:1). Finally, the samples were incubated for 30 minutes and analyzed using the ClarioStar plate-reader.

2.1.2. Culture of a HEK-293T cell line

2.1.2.1. Thawing of HEK-239T cells

HEK293T cells were obtained from ATCC (CRL-3216). Cryovials were retrieved from a -80 °C storage system and thawn on a water bath for 1 minute. Subsequently, the cells were slowly added dropwise to a tube with pre-warmed Iscove's Modified Dulbecco's Medium (IMDM, Cytiva, SH30228-01)) supplemented with 10 % FBS. Next, the tubes were centrifuged at 1600 rpm for 5 minutes and the supernatant was discarded. The cell pellet was resuspended in IMDM + 10 % FBS and the suspension was seeded onto T-25 tissue culture flasks (Corning, #353024) and cultured at 37 °C until passaging.

2.1.2.2. Maintenance of HEK-293T cells

HEK293T cells were passaged every 3-5 days at 70-80 % confluency. Firstly, the cells were washed once with sterile PBS (1X) to remove serum-remnants that may interfere with trypsin activity. To detach the cells, pre-warmed trypsin-EDTA (PUC) solution was added to the wells and the cells were incubated for 2 minutes at 37 °C. Detachment was assisted by gentle tapping on the flask to dislodge remaining adherent cells. Then, the cells were further broken up by aspirating and dispensing with a pipette. Subsequently, IMDM (+10 % FBS) for trypsin inactivation was added to the cells. The suspension was transferred to a tube and centrifuged for 5 minutes at 1600 rpm. After the supernatant was aspirated,the cell pellet was resuspended in fresh IMDM + 10 % FBS and split 1:10 into a T-75 flasks (Corning, #353110) with 10 mL culture medium.

2.1.2.3. Harvesting of HEK-293T cells

Transfected HEK293T cells were harvested for analysis 24 h and 48 h after treatment. The medium for each condition was collected and stored at -20 °C. To collect the cell lysates, pre-warmed TrypLE was added to each well and the cells were incubated for 2 minutes at 37 °C. Next, the cell suspension was collected in a tube and the TrypLE was washed by adding serum-free IMDM. Lastly, the cells were pelleted by centrifugation at 1600 rpm for 5 minutes and, after removing the supernatant, stored at -20 °C until further analysis.

2.1.2.4. Lipofectamine transfection

HEK293T cells were transiently or stably transfected with DNA plasmids encoding NGS Wnt-Fc. Both types of transfections were performed using Lipofectamine 2000 (Invitrogen, 11668-019), while stable transfection additionally required application of the PiggyBac system.

The plasmids used are stated in ***Table 2***.

HEK293T cells were seeded on 6-well plates (Corning, #353046) at 1.5 x 10^5 cells/well and grown in IMDM (+10 % FBS) for 48 h and were transfected at 80 % confluency. The cell number was determined using an automated cell counter (Scepter, C85360).

For transfection, the lipofectamine reagent was diluted 1:25 in serum-free IMDM and incubated for 5 minutes at room temperature. Then, plasmid DNA was diluted in IMDM (4 µg/well). For transfection using the PiggyBac system, the pXL vector was combined with the pSB transposase at a 3:1 ratio and incubated for 10 minutes at room temperature.

Following this, the DNA was combined with the lipofectamine dilution and incubated for 20 minutes at room temperature. After incubation, the medium was removed from the cells and washed once with IMDM to remove any residual serum. The lipofectamine-DNA dilution was added to wells containing 1.5 mL pre-warmed serum-free IMDM and grown for 24 h or 48 h at 37 °C.

2.1.2.5. Zeocin Selection

In order to select cells that had stably integrated the plasmid, transfected HEK293T cells were seeded onto 6-well plates and overlaid with IMDM + 10 % FBS supplemented with Zeocin Selection Reagent (Invitrogen, #45-0430) at a concentration of 50 µg/mL. Zeocin treatment was performed over two weeks. The medium was changed every 2 days.

2.1.2.6. Single-cell clonal selection

To identify single clones displaying high protein expression, HEK293T cells were plated onto 96-well plates for clonal selection after zeocin selection. To achieve this, a starting cell suspension of 2 x 10^4 cells/mL was added to well A1 and serially diluted (1:2) down the first column. These 1:2 dilution steps were repeated across the rows to obtain a serial dilution reaching single cell suspension. In addition, cells were serially diluted onto tissue culture dishes (Corning, #353003) until reaching single cell suspension (1:400). The single cells were cultured for 1-2 weeks at 37 °C until small colonies originating from a single cell had formed. Subsequently, the single cell colonies were expanded onto a 24-well plate using cloning disks (Scienceware, Z374431). To this end, the medium was removed and the cells were washed once with sterile PBS. Then, the disks were soaked in TrypLE for 5 minutes and directly transferred onto the colonies using a sterile forceps. Next, the disks were transferred onto a 24-well plate and, finally, overlaid with IMDM (+10 % FBS).

2.2. DNA cloning

2.2.1. Material

The plasmids used for cloning were obtained as stated in ***Table 2***.

Plasmid	Origin
NGS Wnt Fc (-Koz)	Custom synthesis (Thermo Fisher Scientific)
NGS Wnt-Fc (+Koz)	*established during project*
pXL-BacII-CAG-Zeocin-triple-F2A-MCS	*produced within the facility*
pSB	System Biosciences

Table 2 Plasmid details.

2.2.2. Polymerase chain reaction (PCR)

PCR was performed to introduce nucleic acid motifs into DNA plasmids. The Kozak sequence CACC was introduced into the NGS Wnt-Fc plasmid in order to increase protein expression. Furthermore, restriction sites for AscI and NotI were introduced to enable ligation into the pXL vector. Primers were designed using SnapGene and their sequences are listed in ***Table 3***.

The PCR components were assembled according to ***Table 4***. The PCR reaction was run according to ***Table 5*** for introducing the Kozak sequence and according to ***Table 6*** for introduction restriction sites.

Primer	Sequence
CACC forward	GCAGTGTGTCGGTTTCCATGGTGAAGCTTAAGTTTAAACGCTAGC
CACC reverse	GCTAGCGTTTAAACTTAAGCTTCACCATGGAAACCGACACACTGC
Not1-forward	ATA TCG CGG CCG CCA CCA TGG AAA CCG AC
AscI-reverse	CTC TGG CGC GCC TCA ATG ATG GTG ATG GTG

Table 3 PCR primers.

Sample	Amount
Primer forward (5 µM)	1 µl
Primer reverse (5 µM)	1 µl
dNTPs (100 mM)	1 µl
5X Phusion HF Buffer (#F-518)	10 µl
Phusion polymerase (#F-530S)	0,5 µl
Template	100 ng
$_{dd}H_2O$	*up to 50 µl*
Total	*50 µl*

Table 4 PCR reaction components

PCR step	Temperature [°C]	Duration [minutes]	Cycles
Step 1	98	0:30	
Step 2	98	0:10	35x
Step 3	66	0:15	
Step 4	72	3:30	
Step 5	72	10	

Table 5 PCR programme for the introduction of the Kozak sequence.

PCR step	Temperature [°C]	Duration [minutes]	Cycles
Step 1	98	2	
Step 2	98	0:10	30x
Step 3	62	1	
Step 4	72	2	
Step 5	72	10	

Table 6 PCR programme for the introduction of restriction sites.

2.2.3. PCR purification

The PCR product was purified using the QIAquick® PCR Purification Kit (Qiagen, 28104). The buffers had been previously prepared according to the user's manual. All centrifugation steps were carried out at 17,900 g at room temperature.

First, 5 volumes of Buffer PB were added to the product and mixed by resuspending. Next, the product was transferred to an QIAquick column in a collection tube and centrifuged for 1 minute to bind the DNA. The flow-through was discarded. For washing, Buffer PE was added to the column and centrifugation was repeated for 1 minute. After discarding the flow-through, the column was centrifuged one more time for 1 minute to remove any residual wash buffer. The DNA was eluted by adding 30µL of RNase-free H_2O, shortly incubating at room temperature and finally centrifuging for 1 minute. The DNA concentration was determined by absorbance using a NanoDrop spectrophotometer.

2.2.4. Restriction digest

After the PCR reaction, the template plasmid DNA was removed by digestion with the restriction enzyme DpnI to prepare the PCR product for insertion into the pXL vector plasmid. (AscI, NotI). The restriction enzymes used are mentioned in ***Table 7***.

The reaction components for the digest with DpnI were assembled according to ***Table 8*** and the DNA was digested for 2 h at 37 °C. After digestions, the sample was heated up to 65 °C for 20 minute to inactivate the restriction enzyme.

Restriction Enzyme	Producer	Catalogue Number
DpnI	New England Biolabs	R0176S
NotI	New England Biolabs	R0189S
AscI	New England Biolabs	R0558S

Table 7 Restriction enzymes used for plasmid digestion.

Component	Amount
Plasmid DNA	300 ng-1000 ng
10X Fast digest buffer (Thermo scientific, B64)	2 µ
Restriction enzyme	1 µl
$_{dd}H_2O$	up to 20 µl
Total volume	*20 µl*

Table 8 Restriction digest with DpnI. The NGS Wnt-Fc plasmid was digested after introduction of the Kozak sequence to remove old methylation patterns on the parental DNA.

For plasmid digestion with AscI and NotI a sequential digest was performed to account for differences in buffer requirements (***Table 9***). Firstly, the plasmid DNA, the buffer, AscI and $_{dd}H_2O$ were assembled and incubated at 37 °C for 1 h. Secondly, NaCl and NotI were added and again incubated at 37 °C for 1 h. Finally, the enzymes were heat inactivated at 80 °C for 40 minutes.

Component	Amount
Plasmid DNA	1 µg
CutSmart (New England Biolabs, B6004S)	2 µl
Restriction enzyme	1 µl
NaCl (2M)	1.1 µl
$_{dd}H_2O$	*up to 20 µl*
Total volume	*20 µl*

Table 9 Sequential restriction digest with NotI and AscI.

2.2.5. Ligation

The NGS Wnt-Fc target sequences were inserted into the pXL target vector using ligation. The ligation components were assembled according to ***Table 8***.

Component	Amount
Vector DNA	50 ng
Insert DNA	60.71 ng
T4 DNA ligase reaction buffer (New England Biolabs, B0202S)	2 µL
T4 ligase (New England Biolabs, M0202S)	1 µL
$_{dd}H_2O$	*up to 20 µL*
Total volume	*20 µL*

Table 10 Components for ligation.

2.2.6. Preparation of Luria-Bertani (LB) medium and agar plates

LB medium was prepared by combining LB broth powder (Difco, 214010) with Milli-Q water (1:40) in a bottle and autoclaving for 45 minutes at 121 °C.

For the preparation of agar plates with the desired antibiotic for selection, 6.25 g of LB and 2 g of agar were weighed and combined in a bottle. The bottle was filled up with 250 mL Milli-Q water and autoclaved for 45 minutes. Afterwards, the medium was cooled down at 50 °C and Ampicillin was added to a final concentration of 50 µg/mL. To pour the agar plates, 25 mL of Ampicillin-containing medium was added into petri dishes and shortly cooled down with an open lid to prevent condensation. Once they had polymerized, they were stored at 4 °C.

2.2.7. Bacterial transformation

After heat inactivation, the digested plasmid was introduced into competent *E. coli* HI-106. The cryovials were taken from the -80 °C storage and kept on ice at all times. Ligated DNA (10 ng) was added to the cells and carefully mixed using a pipette. The cells were incubated on ice for 30 minutes. After incubation, the cells were heat-shocked by placing them on 42 °C for 2 minutes. For subsequent recovery, they were immediately put on ice for 2 minutes. Next, sterile LB was added to the vial and the cells were incubated at 37 °C for 1 h. Subsequently, they were pelleted for 1 minute at 5000 rpm and the majority of the supernatant was removed. The cells were resuspended in the remaining supernatant, plated on LB agar plates containing Ampicillin for selection and incubated at 37 °C overnight.

2.2.8. Colony picking and plasmid purification

After transformation, 3-5 of the bacterial colonies were purified for sequence verification. To this end, colonies were picked by gently touching them with a P200 pipette tip and ejecting the

tip into a tube containing LB medium containing Ampicillin. Subsequently, they were incubated at 37 °C overnight, while shaking.

As a next step, the plasmids were extracted and sent for sequencing. To achieve this, the plasmid was purified using the QIAprep® Spin Miniprep Kit (Qiagen, 27104). First, the bacterial overnight culture was pelleted by centrifugation at 6800 g for 3 minutes at room temperature. After discarding the supernatant, the pellet was resuspended in Buffer P1 and transferred to a microcentrifuge tube. Next, the cells were lysed by adding Buffer 2 and the tube was inverted 4-6 times until the solution became clear. To neutralize the reaction, Buffer N3 was added and again mixed by inverting the tubes. After this, the cells were centrifuged for 10 minutes at 17900 g and the supernatant was transferred to a spin column. The column was again centrifuged at 17900 g for 1 minute and the flow-through was discarded. For washing, Buffer PE was added and another centrifugation step at the same settings was performed. Then, the tube was centrifuged again to remove any residual wash buffer. To elute the DNA, the spin column was placed into a tube and 50 µL of RNase-free H_2O were added to the center of the spin column. After incubation at room temperature for 1 minute, the tube was centrifuged at 17900 g for 1 minute and the concentration was determined using Nanodrop.

Finally, the plasmids were prepared at a concentration 100 ng/µL in RNase-free H_2O and sent for Sanger sequencing to Eurofins Genomics.

2.2.9. High copy plasmid purification

The plasmid was isolated using the NucleoBond Xtra Maxi Kit (Macherey-Nagel, 740414.50). In preparation for plasmid isolation, the cells were grown in large-scale liquid culture overnight. The cells were pelleted by centrifugation at 5000 rpm for 1 minute and resuspended in resuspension buffer. To lyse the cells, lysis buffer was added to the cells and the tube was inverted 5 times. Next, the mixture was incubated for 5 minutes at room temperature. Meanwhile, the column and the column filter were equilibrated with equilibration buffer. After incubation, neutralization buffer was added to the tubes and they were inverted until the solution turned colorless. Then, the sample was applied to the column filter and washed one time with equilibration buffer. The filter was discarded and the column was washed once more with washing buffer. Subsequently, the plasmid DNA was eluted with elution buffer and the eluate was collected in a tube. To precipitate the eluted DNA, isopropanol was added to the eluate and the tube was centrifuged at 15000 g for 15 minutes. After discarding the supernatant, 70 % ethanol was added to the pellet for washing. The tube was again centrifuged at 15000 g for 15 minutes and the pellet was dried at room temperature. Finally, the cell pellet was resuspended in RNase-free H_2O and verified by sequencing.

2.3. Electrophoresis and western Blot

2.3.1. Agarose gel electrophoresis

To separate nucleic acids based on their molecular weight, agarose gel electrophoresis was performed. 1 % agarose gels were prepared by combining agarose powder (Sigma-Adlrich, A9539) with 1X TAE buffer (4 mM Tris-acetate, 1 mM EDTA pH 8.5) and heating the flask in the microwave for 2 minutes until fully dissolved. After the gel had cooled down, 3 µL of ethidium bromide were added to enable the visualization of bands. Next, the gel was poured into a casting form of suitable size, where it polymerized for 15 minutes. Then, the gel was transferred to an electrophoresis kit with the comb oriented at the negative pole. The kit was filled with 1X TAE buffer and the comb was carefully removed. The samples were prepared by adding 6X loading dye (New England BioLabs, B7024A) to a final dye concentration of 1X. The GeneRuler 1 kb DNA ladder marker (Thermo Scientific, SM1333) was used as a size reference. The samples were loaded according to loading plan and the program was run at 100 V and 110 mA for 45 minutes. The gel bands were visualized by fluorescence using the Bio-Rad Gel Doc EZ Imager.

2.3.1 Immobilized metal affinity chromatography (IMAC) for the enrichment of HIS-tagged NGS Wnt-Fc

Tetradentate chelating agarose beads (Thermo Scientific, 89966) charged with divalent cobalt (Co^{2+}) were used for enrichment of the His-tagged NGS Wnt-Fc protein. Serum-free medium was collected from HEK293T cells with integrated Kozak-sequence containing NGS Wnt-Fc plasmid after 48 h. To prevent unspecific binding of endogenous proteins with histidine clusters, imidazole (1 M, pH 7.5) was added to reach a final concentration of 10 mM. For protein binding, the agarose beads were added (25 µL/mL) and the tubes were mixed on a rotating wheel for 2 h. After the incubation time, the beads were washed twice for 15 minutes with washing buffer (20 mM Imidazole, 300 mM NaCl in 20 mM Tris PH 8) on a rotating wheel. The tubes were centrifuged for 5 minutes at 500 g between the washing steps. To release the proteins of interest from the beads, two elution steps were performed using two elution buffers (100 mM and 200 mM Imidazole, 150 nM NaCl in 20 mM Tris pH 8) with increased imidazole concentration. The tubes were centrifuged at 1000 g for 5 minutes between the elution steps and the elution fractions were collected for Western blot analysis.

2.3.2 Sample preparation for sodium dodecyl sulphate polyacrylamide gel electrophoresis

Cell lysates and media collected from transfected HEK293T cells were prepared for analysis via sodium dodecyl sulphate polyacrylamide gel electrophoresis (SDS-PAGE) and western blotting. First, the frozen tubes were thawn at room temperature and the cell pellets were

resuspended in lysis buffer (2 % SDS, 150 mM NaCl in 50 mM HEPES pH 8), transferred to smaller tubes and sonicated for 2 minutes (30 % amplitude) to break up the cells via physical disruption. In order to dissolve the SDS that had precipitated during the sonication process, the tubes were warmed to 37 °C and shortly centrifuged. As a next step, the cell lysates and media samples were prepared for SDS-PAGE by diluting the desired sample volume in 4X Laemmli sample buffer (Biorad, 1610747) to a final buffer concentration of 1X. Finally, the samples were inactivated at 95 °C for 5 minutes and shortly centrifuged prior to loading.

2.3.3 SDS-PAGE

The prepared samples were separated according to their molecular weight during SDS-PAGE. Pre-cast 1.0 mm gels (Invitrogen, XP04205BOX) were assembled in the SDS-PAGE kit and the tank was filled with 5X running buffer (25 mM Tris, 192 mM glycine, 0.1% SDS) to approximately ¾ of the total volume. Before sample loading, the 10- or 15-slot comb was removed and the wells were rinsed using a syringe to remove any potential remnants blocking the lanes. Additionally, any air bubbles that might interfere with the electrophoresis were removed. Next, the samples as well as the protein ladder (Biorad, 1610376), serving as a reference for molecular weight, were loaded. The SDS-PAGE was run at a constant 180 V for 45 minutes to 1 h.

2.3.4 Western Blot

Western blotting was performed to transfer the proteins separated during SDS-PAGE onto a membrane, to enable chemiluminescence- or fluorescence-based detection. Before blotting, the PVDF membrane (Millipore, IPVH00010) was first soaked in 100 % methanol and then transferred to Turbo Transfer buffer (Biorad, 1704727) + 20 % ethanol for 20 minutes. Similarly, the filter paper was wet in Turbo transfer buffer + 20% ethanol before assembling the blotting system. After having carefully removed the gel from the SDS-PAGE kit, the blotting sandwich was assembled by orderly layering the pre-wet filter paper, the membrane, the gel and another layer of filter paper on a cathode plate. A blot roller was used to remove any bubbles and the resulting liquid was poured off prior to starting the system. The program was run for 25 minutes at 1.0 A and 20 V. After transference, unspecific binding sites on the membrane were blocked in 2-3 % BSA in TBS-T for 1 h at room temperature or overnight at 4 °C and subsequently incubated with the primary antibody (Qiagen Mouse Anti-His, #34660, 1:1 000) in 3 % BSA in Tris-buffered saline with Tween (TBS-T) for 2 h at room temperature or overnight at 4 °C. Subsequently, the primary antibody was removed by washing three times with TBS-T for 15 minutes. Following this, the membrane was incubated with the secondary antibody for 2 h. For chemiluminescent detection, horse-radish peroxidase- (HRP) conjugated secondary Goat Anti-Mouse IgG (SouthernBiotech, 1030-05, 1:5000) in 3% BSA in TBST was used. For

fluorescent detection, Donkey anti-Mouse IgG (H+L) Highly Cross-Adsorbed Secondary Antibody, Alexa Fluor™ 680 (Thermo Scientific, A10038, 1:5000) was used. After incubation, the membrane was again washed three times with TBS-T for 15 minutes and, additionally, once with PBS for 15 minutes to remove any Tween-remnants.

For chemiluminescent detection, the chemiluminescent HRP substrate (Millipore, WBKLS0500) was prepared (1:1), added onto the membrane and covered with a plastic foil. Pictures were taken using the ImageQuant Las 4000 mini Biomolecular Imager. For fluorescent antibodies, the Li-Cor Odyssey Clx Infrared Fluorescent Western Scanning/Imaging System was used.

2.4. Mass spectrometry

Mass spectrometry was performed in order to determine the protein levels of colonic organoid cultures 48 h after cytokine treatment. To this end, Corning cell recovery solution (Sigma-Aldrich, CLS354253) was pipetted onto the wells and the BME was carefully scraped off, holding the plate at an 45° angle. Next, the suspension was transferred to clean tubes and incubated for 1 h at 4 °C on an end-over-end rotator. Subsequently, the tubes were spun down for 5 minutes at 400 g at 4 °C. The supernatant was aspirated and the pellet was resolved in cold PBS. Next, the tubes were centrifuged at 400 g twice and the supernatant was removed. As a following step, the pellet was resolved in lysis buffer (2 %SDS, 150 mM NaCl and 50 mM HEPES pH 7.4) and the tubes were shaken at 1000 rpm for 15 minutes. After this, the samples were sonicated for 4 minutes in order to shred the DNA. Then, the samples were reduced with 5 mM TCEP for 15 minutes at 50 °C and, subsequently, alkylated with 20 mM 2-CAA for 30 minutes at dark. Next, SP3 magnetic beads (Cytiva, 6152105050250) were added to a defined amount of protein input (1:10) and an equal amount of 80 % ethanol was added. The samples were put on a thermal shaker for 10 minutes at 1000 rpm, after which the supernatant was aspirated. Next, 80 % ethanol was added once more and the tubes were placed back on the thermal shaker for 5 minutes. This procedure of ethanol addition was repeated at least twice. The samples were placed on a magnetic rack and washed a final time with 80 % ethanol. Then, 10 mM ammonium bicarbonate (pH 7.4) and Lys-C/Trypsin (1:100) were added to the tubes. After this, the samples were kept shaking at 37 °C overnight. On the next day, the tubes were put on a magnetic rack for 5 minutes and the supernatant was transferred to new tubes as the first eluate. Then, Milli-Q water was added to the samples and the tubes were shaken for 10 minutes at 1000 rpm. Next, they were centrifuged at 1 000 g for 1 minute and, subsequently, put on the magnetic rack for 5 minutes. The supernatant was combined with the first eluate. Finally, the peptides were lyophilized, resolved in 0.5 % TFA and analyzed by mass spectrometry.

3. Results

3.1. Identification of cytokines regulating stem cell differentiation into goblet cells

The mucus covering the intestinal tract forms a selective barrier that limits the access of microorganisms to the underlying epithelium, thereby exerting a protective function. Mucus-producing goblet cells play an important role in gut health and disease by maintaining the homeostasis of the intact intestinal barrier function. Goblet cell function is tightly regulated by immune cell-derived cytokines and alterations in immune responses have been shown to be implicated with inflammatory conditions, including IBDs (Gustafsson & Johansson, 2022). Hence, studying the impact of immune factors on the differentiation of ISCs into goblet cells is essential for extending our knowledge of their role in infection. To identify drivers of goblet cell differentiation in the colon, redMUC2 organoid cultures expressing mCherry-labelled MUC2, a prominent goblet cell marker, were treated with selected cytokines 48 h after seeding and differentiation was induced for 72 h. Differentiation was assessed by the fluorescence-based determination of MUC2 levels, while cell proliferation was measured in luminescent assays (***Figure 5A***).

3.1.1. Assay optimization

The outcome of luminescent and fluorescent assays largely depends on the tissue cultures plates chosen. While white plates are usually preferred for luminescent assays because they maximize the light output signal, black plates pose the advantage of reducing background signal in fluorescent assays. As the differentiation state and the cell growth rate were determined in a combined setup, there was a need to optimize the assay conditions by testing white and black plates with the aim of minimizing background signal, while maintaining a high luminescent output.

As shown in ***Figure 5B***, the background signal in fluorescent assays is reduced considerably when using black plates compared to white. While the background signal in white plates exceeded the actual signal emitted from the organoid cultures, the use of black plates enabled a much better discrimination between the background and the cultures. Furthermore, although white plates yielded a higher output signal in luminescent assays, the signal was only slightly decreased when using black plates. Hence, black plates should be used to optimize for light output and background signal.

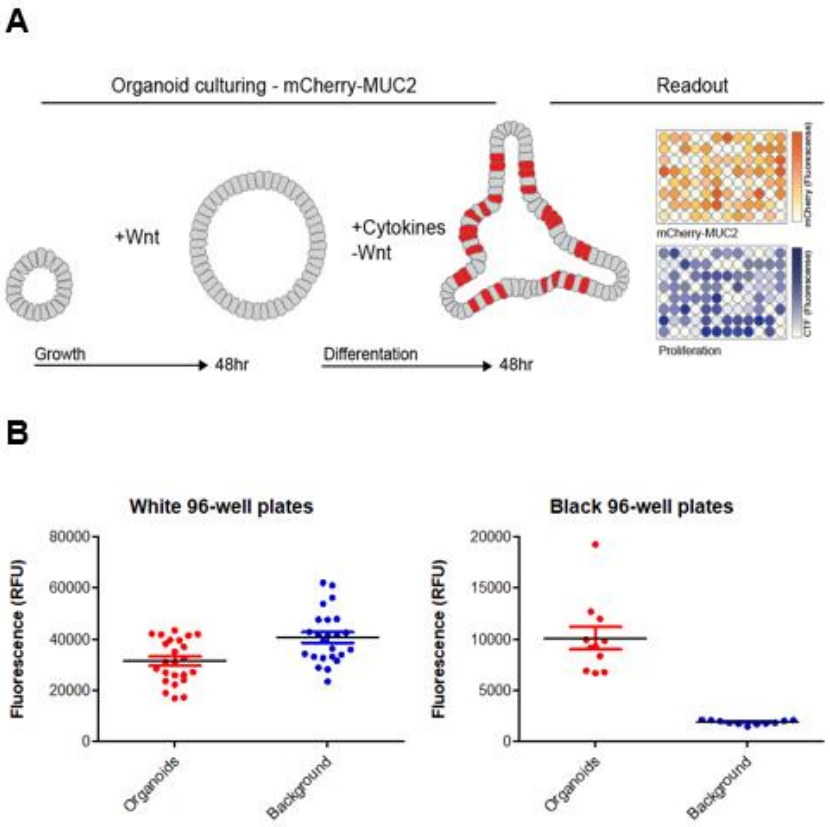

Figure 5 Differentiation assay of redMUC2 colonic organoid cultures. A) Assay setup for the fluorescence-based detection of goblet cell differentiation and luminescence-based determination of cell proliferation. **B)** Comparison of relative fluorescent units (RFU) obtained from organoids grown on white and black plates.

3.1.2. Microscopy analysis of differentiating organoids

Undifferentiated organoids are characterized by a light color and round shape in microscopy images, while differentiated organoids show a transition to dark color and apical-basolateral morphology changes. This difference in organoid morphology is depicted in ***Figure 6***. As undifferentiated cells maintain a higher proliferation rate than differentiated cells, a higher degree of morphological changes and a reduced cell growth can be correlated with an earlier onset of differentiation. In the following, the effect of cytokine treatment on differentiation and proliferation of redMUC2 organoid cultures was assessed using different microscopy techniques.

Figure 7 shows organoid cultures imaged using phase contrast microscopy. The results demonstrate that transitioning to Wnt-lacking ENR culture medium effectively induced differentiation, while cells grown in stem cell-maintaining WENR continued to stay in stem cell phase. Organoids grown in ENR without cytokine treatment were used as a reference for baseline differentiation. Furthermore, treatment with goblet cell differentiation-inducing DAPT was used as a positive control.

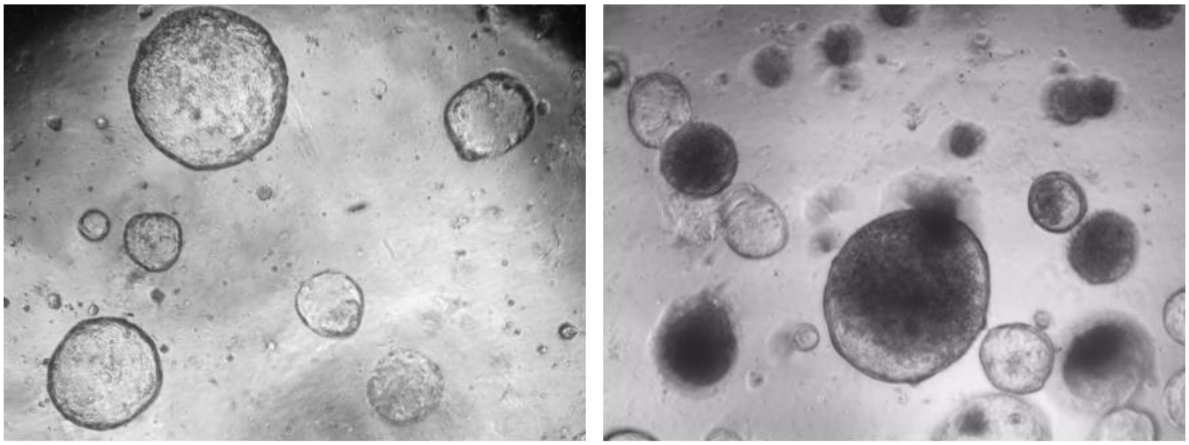

Figure 6 Comparison of the morphology changes in undifferentiated and differentiated organoids. Undifferentiated organoids (*left*) display a cystic morphology, indicated by a light color and round shape. Upon differentiation, organoids obtain a budding shape (*right*), characterized by a dark color and small outgrowths.

Overall, the results reveal that differentiation was induced to varying extents in all treatment conditions. All cultures displayed a shift to a differentiating morphology, although to a lesser degree in organoids stimulated with IL-17A. Notably, stimulation with IL-13, IFN-γ and IL-22 obtained higher degrees of budding, while organoids treated with TNF-α, IL17A and IL-10 showed a rounder shape, similar to the ENR control. An important observation is that organoids treated with IL-13 and IFN-γ were inhibited in their growth, with the organoid size resembling the positive control, suggesting a strong differentiation-promoting effect. Interestingly, this reduction in growth was not observed in IL-22-stimulated cultures. Moreover, treatment with IFN-γ displayed high degrees of shedding, indicative of cell death.

As a next step, fluorescence microscopy was used to study whether cytokine stimulation induces organoid differentiation into goblet cells or another cell lineage, such as enterocytes. To achieve this, the mCherry-signal produced by goblet cell-specific MUC2 expression was visualized. As depicted in ***Figure 8***, differentiation was suppressed in organoids grown in stem cell-maintaining WENR medium, while cultures grown in the absence of Wnt started differentiating (ENR). Differentiation into goblet cells was observed for all treatment conditions, with IL-13 and IL-22 producing higher mCherry signal, compared to organoids treated with TNF-α, IL-17A, IFN-γ. Notably, the signal in for IL-13 and IL-22 seems to be lower than the baseline signal observed in ENR cultures. However, the cell density during fluorescence imaging was low, likely influencing the experimental outcome.

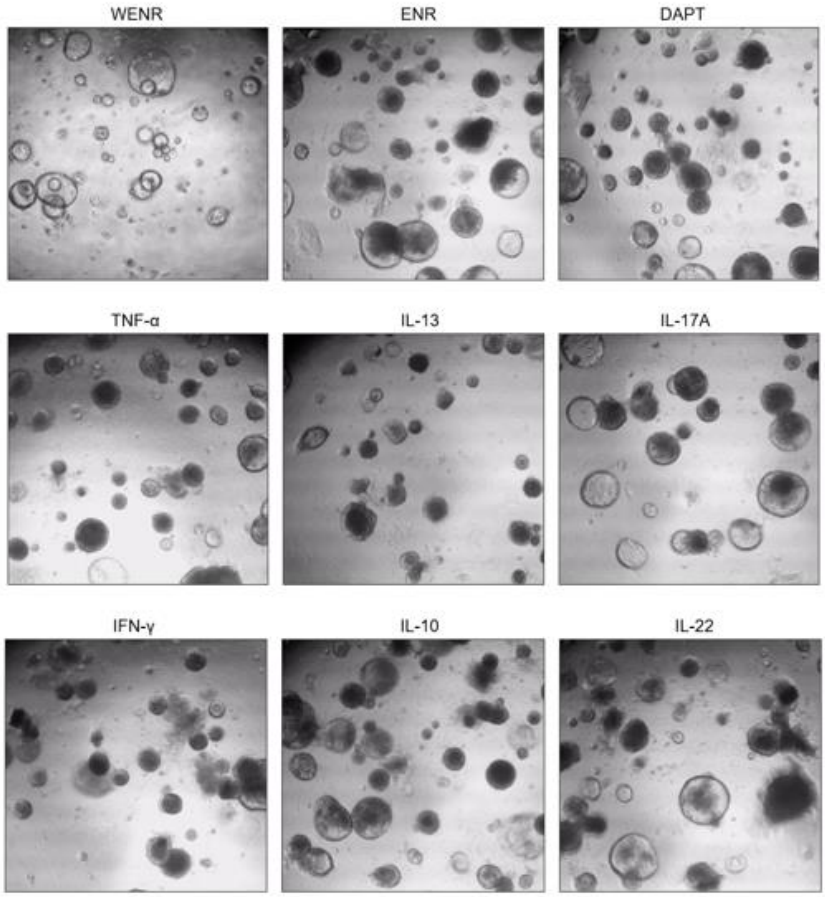

Figure 7 Organoid differentiation upon cytokine stimulation under the light microscope. Transition from Wnt-containing WENR (**W**nt, **E**GF, **N**oggin, **R**-spondin) to Wnt-lacking ENR medium induced a shift of cystic to budding organoids. The Notch-signalling inhibitor DAPT was used as a positive control for goblet cell differentiation.

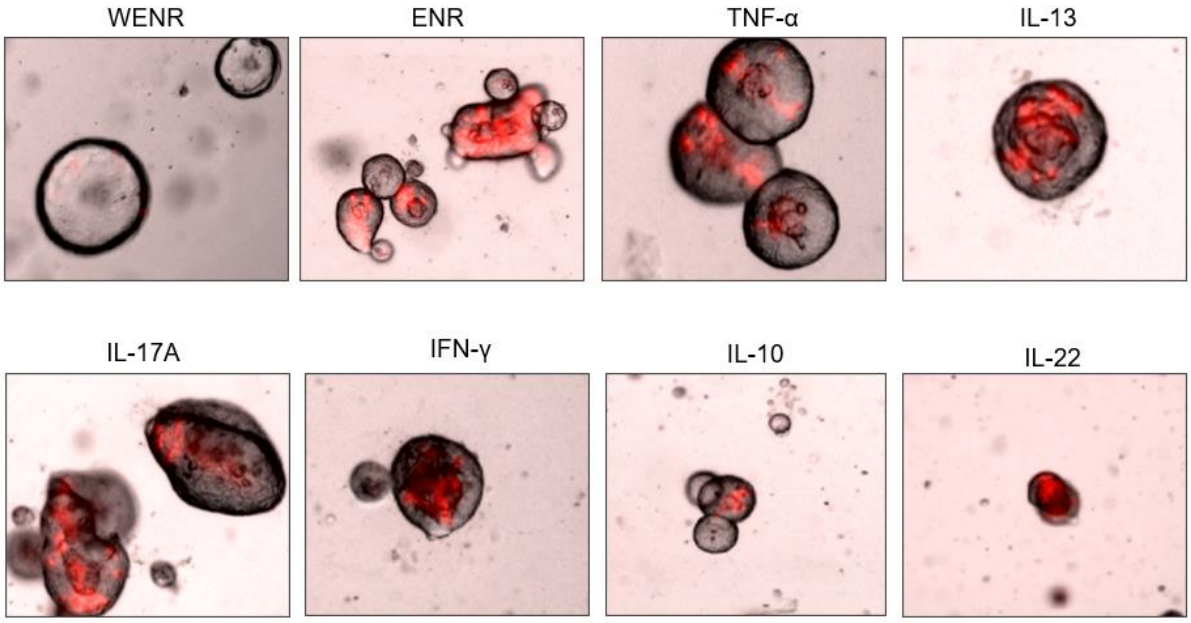

Figure 8 Fluorescent microscopy images of colonic organoids expressing mCherry-labelled MUC2.

3.1.3. Determination of goblet cell differentiation in fluorescent assays

The analysis of morphology and MUC2-expression gave first insights into the differentiating effects of cytokine treatment on colonic organoids. In order to study this further, differentiation and proliferation were analyzed by quantifying the mCherry-signal and the cell growth rate in fluorescent and luminescent assays respectively. Analogous to the microscopy analysis, the ENR signal was used as a baseline for differentiation, while DAPT was used as a positive control.

As shown in ***Figure 9A***, differentiation was induced to different extents upon cytokine treatment. As expected from the microscopy observations, organoid cultures stimulated with IL-13, IFN-γ and IL-22 displayed a significantly increased fluorescent signal compared to ENR, with a 1.6-fold, 2.5-fold and 1.7-fold increase respectively. Strikingly, IL-13 induced differentiation even in the presence of Wnt, displaying a 2.5-fold increase in mCherry signal when administered in 50CM (***Figure 9C***). Furthermore, treatment with TNF-α, IL-17A and IL-10 yielded signals comparable to the baseline.

The results obtained for cell proliferation show that cell growth was highest under undifferentiated conditions (WENR) and only very slightly decreased under baseline differentiation (ENR) (***Figure 9B***). Notably, cell growth was strongly affected upon treatment with IL-13, IFN-γ and IL-22 stimulation, indicative of an early onset of differentiation. It is important to note that the high mCherry-signal obtained for IFN-γ in combination with a strongly impaired growth rate and shedding events is indicative of cell death, resulting in autofluorescence likely impacting the assay readout. This effect was further assessed in ***Chapter 3.1.5***. Furthermore, treatment with TNF-α, IL-17A and IL-10 display growth rates comparable to ENR.

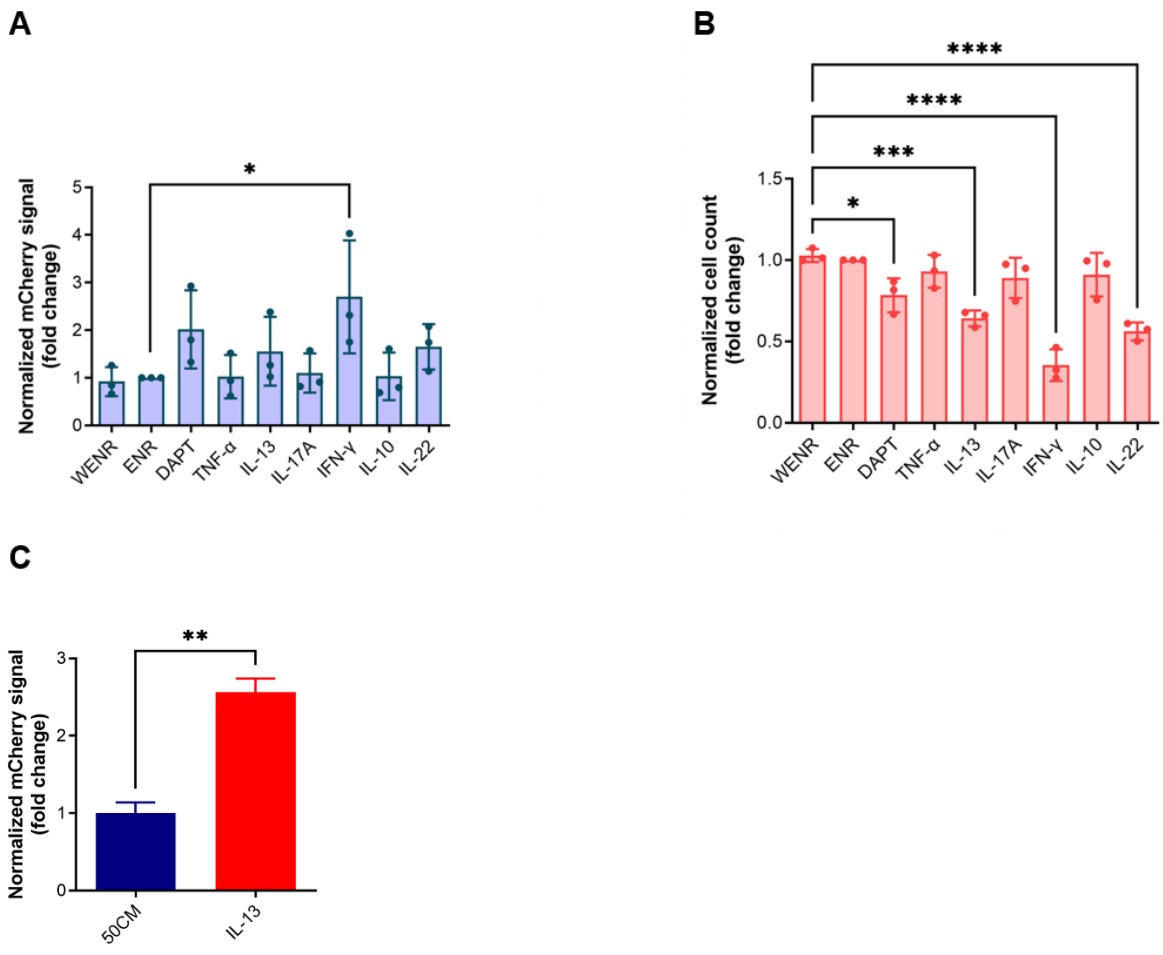

Figure 9 Quantification of mCherry-expressing MUC2 abundance and cell growth in colonic organoids. **A)** Fold change of mCherry-signal upon cytokine stimulation normalized to cell number. **B)** Fold change of the cell count normalized to the control (ENR). One-way ANOVA with Dunnett's multiple comparisons test, * *p<0.05*, *** *p<0.001*, **** *p<0.0001*. **C)** Normalized mCherry signal of IL-13 administered in 50CM. Unpaired t test, ** *p<0.01*.

3.1.4. Analysis of goblet cell differentiation on a protein level

In order to further investigate the role of cytokines on goblet cell differentiation, differentiation was assessed at protein level. To this end, changes in the expression levels of the goblet cell markers MUC2, FCGBP and CLCA1 were studied using mass spectrometry.

The results are depicted in ***Figure 10***. In support of the previous findings, expression of MUC2, FCGBP and CLCA1 was significantly upregulated in IL-13-treated samples, displaying an approximately 18-fold increase for MUC2 and 34-fold increase for FCGBP. As expected, no upregulation was observed for TNF-α, IL-17A, IFN-γ and IL-10. This further suggests that IFN-γ is not involved in driving differentiation, but rather in inducing cell death. Interestingly however, IL-22 did not show an increase in goblet cell marker expression levels.

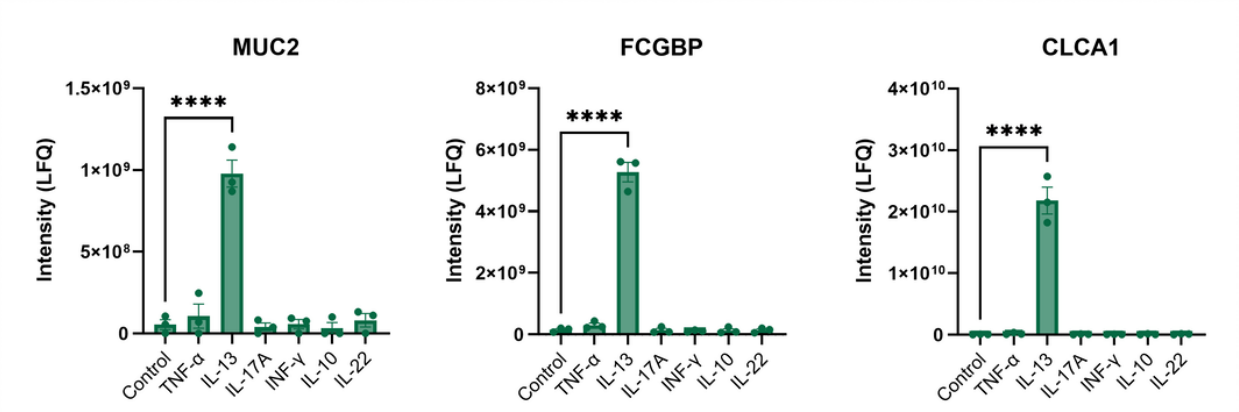

Figure 10 Cytokine-mediated expression of goblet-cell markers in colonic organoid cultures. Label-free protein abundance is represented as the normalized peak intensity (LFQ) for each individual treatment for MUC2, FCGBP and CLCA1. One way ANOVA with Dunnett's multiple comparisons test, **** *p<0.0001.*

3.1.5. Cytotoxicity assay

Our previous data has suggested cytotoxic effects for IFN-γ on colonic stem cells. In order to further study this, organoid cultures were treated with cytokines 24 h after seeding in 50CM and cytotoxicity was assessed after a total of 72 h. As a positive control for cell death, Triton-X was used to induce cell lysis.

As demonstrated in ***Figure 11***, cytotoxicity was slightly increased upon treatment with IL-13 and IFN-γ. TNF-α, IL-17A and IL-22 display similar values to the 50CM control. Notably, cytotoxicity was assessed under undifferentiated conditions, while strong impairment of cell growth upon IFN-γ was mainly observed during differentiation in ENR.

To summarize, the results obtained from microscopy imaging and fluorescent assays identified IL-13 and IL-22 as a strong differentiation driver of goblet cell differentiation in colonic stem cells. Furthermore, the goblet cell markers MUC2, FCGBP and CLCA1 were shown to be highly upregulated upon IL-13, which was not found for IL-22. Interestingly, IL-13 even induces differentiation in Wnt-containing culture medium, indicating that an implication in overwriting stem cell-maintaining mechanisms. Finally, a potential cytotoxic effect during differentiation was observed for IL-13 and IFN-γ.

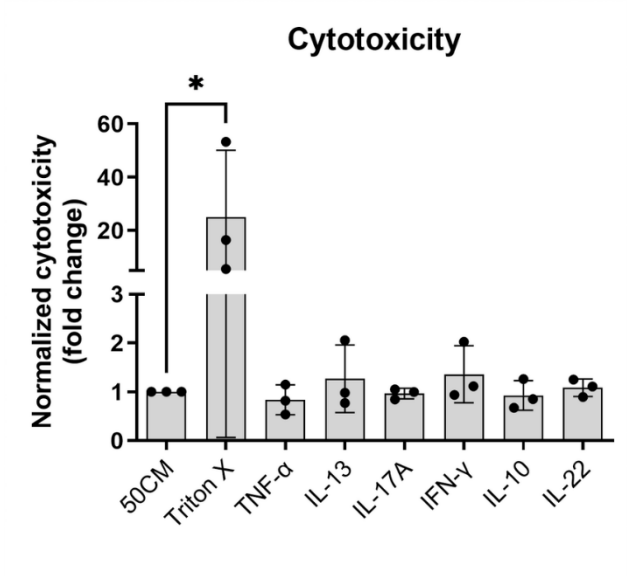

Figure 11 Determination of cytotoxic effects of cytokine treatment on colonic organoid cultures. One way ANOVA with Dunnett's multiple comparisons test, * *p<0.05*.

3.2. Determination of NOX1-mediated ROS production upon cytokine stimulation of colonic organoid cultures

Self-renewal, proliferation and differentiation of the intestinal epithelium is supported by redox-dependent modulation of essential signaling pathways through the action of NOXs. In the colon, NOX1-generated ROS modulates the activation of EGFR in cycling colonic stem cells, forming a connection between ROS production and cell proliferation (Van Der Post et al., 2021). The production of ROS by colonic stem cells is tightly regulated and can be modulated in response to cytokine signaling produced by gut-resident immune cells. High concentrations of ROS have the potential to impair the epithelial barrier and induce mucosal inflammation as well as oxidative stress associated with the progression of IBD. However, at physiological concentrations, ROS are involved in a range of beneficial processes, including mucosal wound healing, tissue repair and fighting invading pathogens by antimicrobial defense mechanisms, ultimately enhancing cell survival (Sahoo et al., 2023).

To gain further insights into the potential correlation of ROS production and cell proliferation, colonic organoid cultures were treated with a library of selected cytokines relevant for the intestinal epithelium and NOX1-derived ROS production as well as the cell growth rate were determined in order to expand our understanding of the physiological role of ROS in colonic stem cell homeostasis.

3.2.1. Assessment of ROS production and cell proliferation in GF and ConvR organoid cultures

The immune response in the intestine is largely shaped by interactions with the gut microbiome and its derived metabolites. A lot of our current knowledge of intestinal biology was obtained through the study of germ-free (GF) mice, i.e. sterile mice that are devoid of microorganisms. GF mice exhibit significant differences in both their innate as well as their adaptive immunity compared to mice that were conventionally raised (ConvR). Overall, their immune system is more immature, showing reduced numbers of Peyer's patches and epithelial lymphocytes, leading to differences in inflammatory responses due to the lack of immune modulation via the gut microbiome (Suriano et al., 2022). In the following, the effects of cytokine treatment on colonic organoid cultures from GF and ConvR mice were studied in order to gain insight into the mechanisms regulating ISC fate in response to external stimuli. More specifically, cell proliferation was assessed in relation to ROS production, in order to expand our understanding of the adaptive mechanisms to the gut microbiome during early life and how this exposure shapes immune responses. To this end, GF and ConvR organoid cultures were treated with the respective cytokines 24 h after seeding and cell proliferation and ROS were determined after 48 h using a combination of fluorescence- and luminescence-based assays. Importantly,

the detection of ROS is based on oxidation of the L-012 probe, thereby measuring the generation of extracellular superoxide.

The results for ROS production and cell proliferation are depicted in ***Figure 12***. ROS production was significantly decreased upon IL-13 stimulation (***Figure 12A***). Moreover, ROS generation was increased upon treatment with IL-17A, IFN-γ and IL-22. Interestingly, the ROS response to IFN-γ in GF organoid cultures displayed a >2-fold increase, while the levels in ConvR cultures were comparable to the control. In contrast, the response to IL-17A was reduced from a 4-fold increase in ConvR organoids to 3-fold in GF cultures. IL-22 stimulation yielded a similar increase of ROS (>2-fold) in both cultures, while TNF-α and IL-10 showed levels comparable to the baseline. The ROS response overtime for IL-13, IL-17A and IL-22 is depicted in ***Figure 13***.

In line with this observation, cell proliferation was significantly impacted upon treatment with IL-13, whereas the other cytokines displayed a similar cell growth to the control (50CM) (***Figure 12B***). GF cultures displayed a reduced growth rate upon stimulation with TNF-α, IL-13, IL-10 and IL-22 compared to ConvR, while treatment with IL-17A and IFN-γ yielded similar results in both culture models. Notably, treatment with IL-13 yielded a 2-fold decrease in cell growth for GF cultures and an approximately 1.5-fold decrease for ConvR.

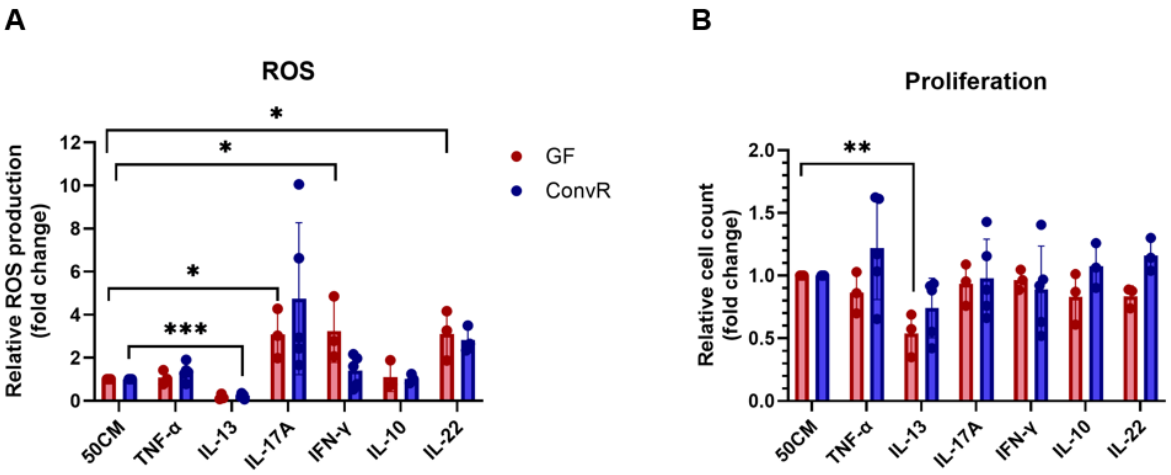

Figure 12 Cytokine stimulation of GF and ConvR colonic organoid cultures. A) Relative ROS generation and **B)** relative cell count of GF and ConvR organoid cultures upon cytokine stimulation. One way ANOVA with Dunnett's multiple comparisons test, * *p<0.05, ** p<0.01, *** p<0.001.*

Overall, these results show that ROS production is altered in response to stimulation with IL-13, IL-17A, IFN-γ and IL-22 in GF as well as ConvR organoid cultures. The magnitude of the response differs in GF and ConvR cultures treated with IL-17A and IFN-γ, with GF cultures being more responsive to IFN-γ stimulation, while showing a reduced response to IL-17A. This shows potential implications in the adaptive mechanisms to these cytokines upon microbial

modulation. Furthermore, IL-13 was identified as an inhibitor of ROS production, which is further reflected in organoid proliferation.

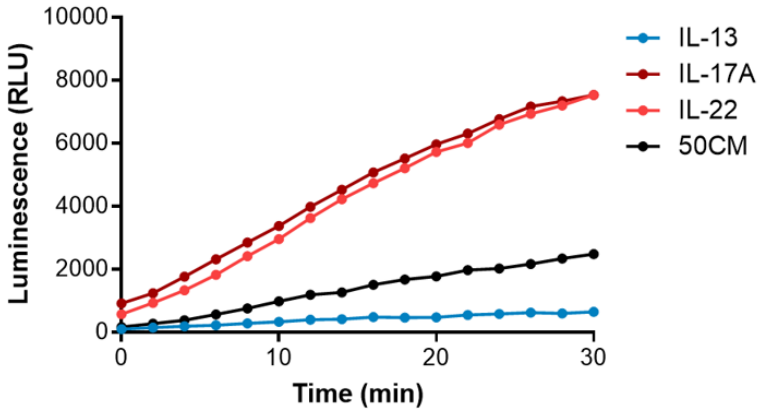

Figure 13 Differences in the magnitude of the ROS response upon cytokine stimulation in ConvR organoid cultures. The luminescent signal correlates with the production extracellular ROS and was measured over 30 minutes.

3.2.2. Analysis of ROS production on a proteomic level

In addition to the determination of extracellular ROS in luminescent assays, the effect of cytokine stimulation in colonic organoid cultures was studied on a protein level in order to gain further insights into the enzymatic source of ROS. To this end, mass spectrometry was performed on ConvR organoids 48 h after cytokine treatment.

The analysis of the proteomics data reveals that cytokine stimulation affected regulation of NADPH oxidases of the NOX/DUOX family, more specifically NOX1, DUOX2 and NOS2. NOX1 activity mainly produces superoxide, while the main ROS product of DUOX2 is hydrogen peroxide. NOS2-derived nitric oxide was not determined in the luminescence assay. Importantly, NOX1 activity has been shown to be specific for stem cells, while DUOX2 is also associated with differentiating cell types.

As shown in ***Figure 14***, NOX1 and DUOX2 expression were significantly upregulated in IL-17A-treated samples, supporting the results obtained from the luminescent assays (***Chapter 3.2.1***). Furthermore, NOS2 was highly upregulated in response to IFN-γ stimulation, while NOX1 and DUOX2 were not affected. This is in accordance with our previous data, in which the nitric oxide was not detected. Notably, IL-13 and IL-22 caused a significant downregulation of NOX1, while DUOX2 was upregulated upon treatment, which further supports the findings identifying IL-13 and IL-22 as drivers of goblet cell differentiation (***Chapter 3.1***). Interestingly however, IL-17A shows an upregulation of enzymes, implicating a dual role of ROS production.

Moreover, IL-22 was upregulated in NOS2, while IL-10 and TNF-α yielded similar results to the control (50CM).

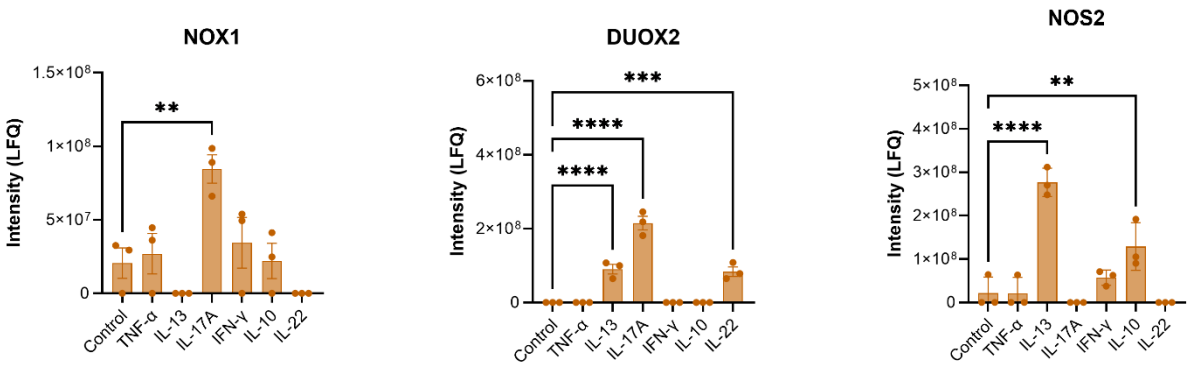

Figure 14 Expression of NOX/DUOX family members upon cytokine stimulation in colonic organoid cultures. Protein identification and label free quantification (LFQ) by mass spectrometry are based on the relative abundance for each protein per treatment. One way ANOVA with Dunnett's multiple comparisons test, ** *p<0.01,* *** *p<0.001,* **** *p<0.0001.*

In addition to ROS expression, alterations in cell growth in response to cytokine treatment were studied based on different expression levels of proteins involved in cell division. ***Figure 15*** displays prominent proliferation markers (MKI67, PCNA, CDK1) and changes in their regulation after cytokine stimulation. Overall, IL-13 and IL-17A caused a significant downregulation of all marker proliferation markers. More precisely, IL-13 caused a >3-fold decrease of MKI67 and CDK1, as well as a >2-fold decrease of PCNA, while the decrease was slightly lower upon IL-17 stimulation. Furthermore, the expression of PCNA was significantly decreased upon IL-22 stimulation, while MKI67 and CDK1 levels were similar to the control. Moreover, TNF-α, IL-10 and IFN-γ did not have significant effects on the cell growth.

In conclusion, these results suggest IL-13 and IL-22 as potent inhibitors of NOX1-induced ROS production, as well as differentiation-associated DUOX2-upregulation. Furthermore, IL-17A is involved in NOX1- and DUOX2-regulation, calling for further studies elucidating its extensive role in ROS production. Importantly, a reduction in NOX1-derived ROS correlates with reduced expression of proliferation markers in IL-13-treated samples, whereas this correlation was only partly found for IL-22. Moreover, increased production of NOX1-derived ROS correlated with decreased proliferation in IL-17A-treated organoids.

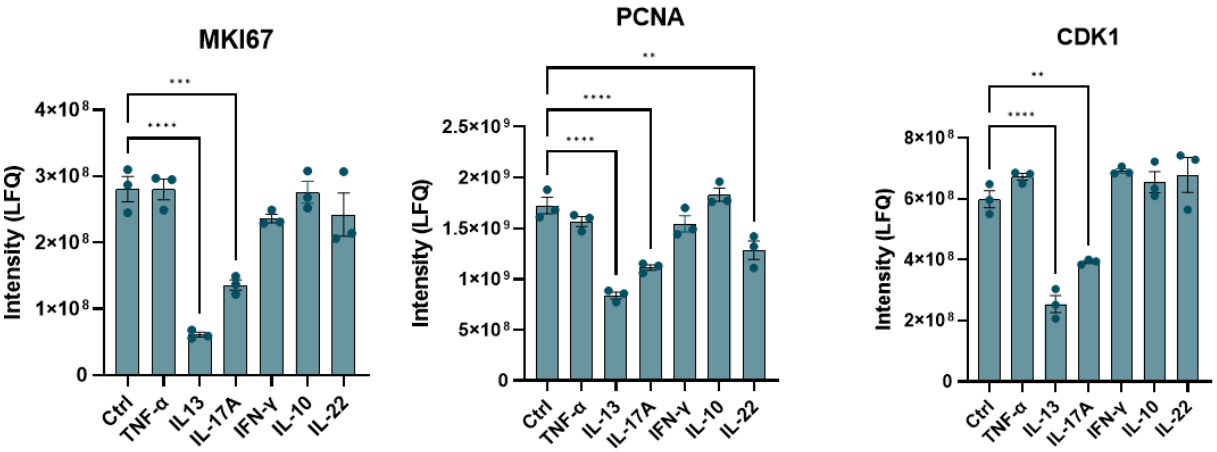

Figure 15 Regulation of proliferation markers (MKI67, PCNA, CDK1) upon cytokine stimulation of organoid cultures. One way ANOVA with Dunnett's multiple comparisons test, ** *p<0.01, *** p<0.001, **** p<0.0001.*

3.2.3. Assessment of ROS production in a concentration-dependent manner

The biological effect of ROS in the intestinal tract is likely dose-dependent and regulated by the abundance of each specific cytokine receptor. To study the effect of different cytokine concentrations on the generation of ROS and the impact on cell proliferation, ConvR colonic organoids were treated with selected cytokines at a range of different concentrations (10 ng/mL-100 ng/mL) for 48 h. Subsequently, ROS production and cell number were determined.

The results show a concentration-dependency of ROS production in organoid cultures upon cytokine stimulation for some cytokines, while others seem to lack this dose-dependent effect (***Figure 16***). The ROS response to stimulation with TNF-α and IFN-γ occurs in a concentration-dependent manner, while production in IL-13-, IL-17A-, IL-10- and IL-22-treated cells is more constant (***Figure 17***). More specifically, ROS production in TNF-α increases consistently with increasing concentration, until a plateau is reached at 75 ng/mL, suggesting that receptor-saturation is attained at this point. Interestingly, ROS production upon stimulation with IFN-γ shows the opposite effect, with ROS levels steadily decreasing with increasing concentration, following a pattern of receptor desensitization. Furthermore, IL-17A and IL-22 yielded increased ROS levels (2-2.5-fold change) at all concentrations, whereas levels in IL-10 stimulated cultures showed no difference to the control (50CM). Notably, stimulation with IL-13 yielded a significant decrease in ROS at all concentrations, presenting a very potent inhibitory effect.

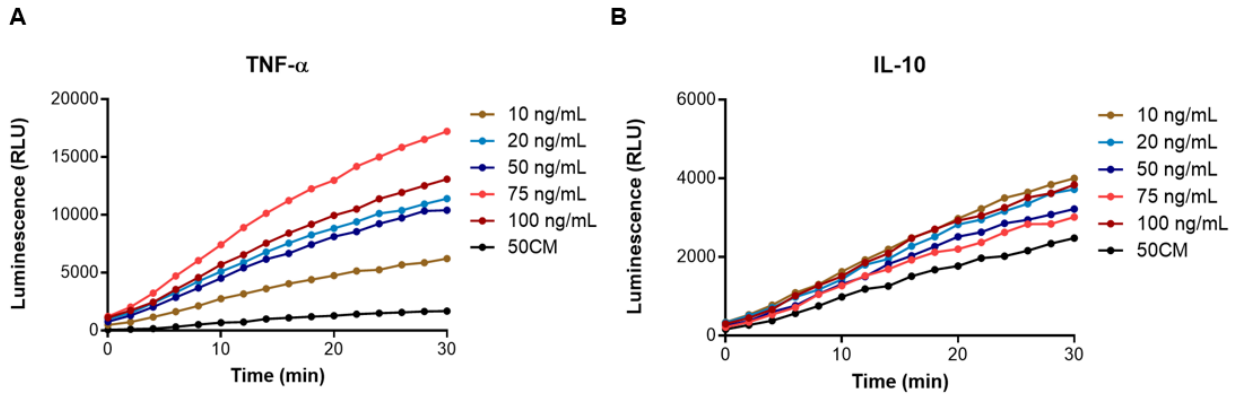

Figure 16 ROS production in colonic organoids upon stimulation with different concentrations of TNF-α and IL-10. A) The maximal response in TNF-α occurred at 75 ng/mL, the minimal response at 10 ng/mL, showing a fold change of 2.77. **B)** The response in IL10-stimulated cultures was highest at 10 ng/mL and lowest at 75 ng/mL (1.3-fold change).

To expand on this, the dose-dependent effect of ROS generation was studied with regards to alterations in cell proliferation (***Figure 18***). Overall, organoid proliferation was similar to the control for all conditions. As expected, constant ROS production by IL-13, IL-17A, IL-10 and IL-22 stimulation did not show a concentration-dependent impact on cell proliferation. Notably, stimulation with IL-13 yielded slightly decreased cell proliferation. Furthermore, the dose-dependent effects in ROS production upon TNF-α and IFN-γ treatment were not reflected in cell number. It is important to note that high cytokine doses did not negatively affect cell growth, suggesting that cytokines do not have a cytotoxic affect at these concentrations.

To summarize, ROS generation occurs in a concentration-dependent manner upon stimulation with TNF-α and IFN-γ, while this dose-dependency was not seen in IL-13, IL-17A, IL-10 and IL-22. Furthermore, cell proliferation was not significantly impacted by different cytokine concentrations, suggesting that the applied doses neither upregulate cell proliferation nor impair cell growth.

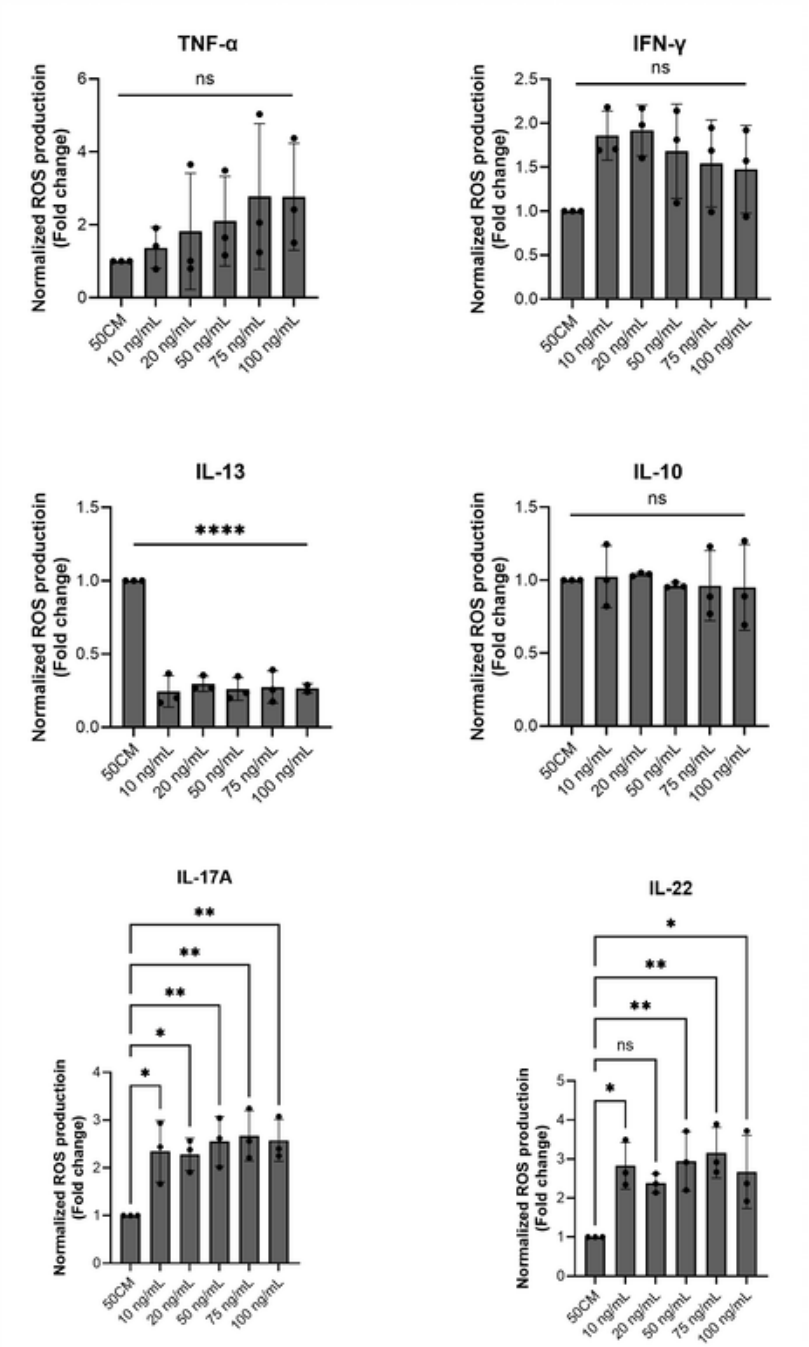

Figure 17 ROS production in intestinal organoids upon stimulation with varying cytokine concentrations. ROS production in TNFα and IFN-γ is dose dependent. TNFα steadily increases with increasing concentration, while IFN-γ steadily decreases. Generation of ROS upon stimulation with IL13, IL17a, IL10 and IL22 does not display a concentration-dependent effect. One way ANOVA with Dunnett's multiple comparisons test, * *p<0.05*, ** *p<0.01, **** p<0.0001.*

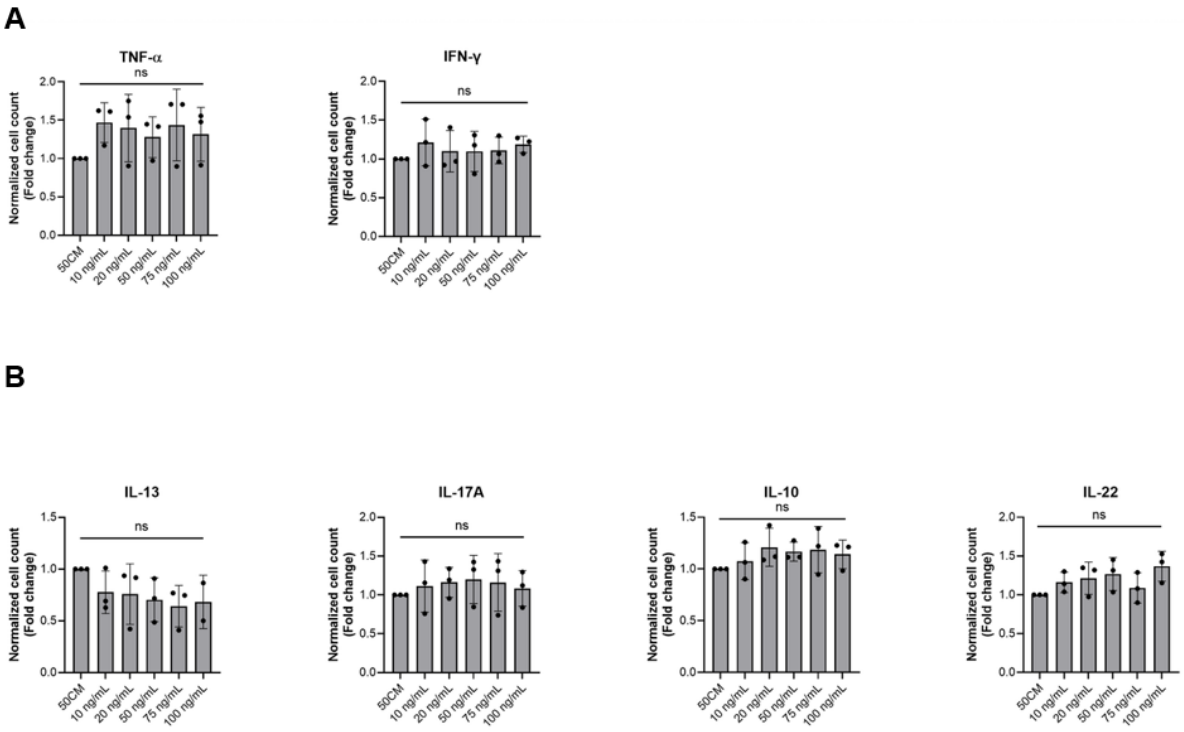

Figure 18 Cell proliferation upon cytokine stimulation at varying concentrations. A) Cell proliferation for cytokines displaying a dose-dependent production of ROS. **B)** Cell count for cytokines without a concentration-dependent effect on ROS. One way ANOVA with Dunnett's multiple comparisons test. * $p<0.05$

3.2.4. Assessment of the time-dependent production of ROS upon IL-17A stimulation

The generation of ROS as well as their effect on physiological processes are often transient, owing to their high reactivity within a biological context (Sies et al., 2022). Hence, it is crucial to further elucidate the temporal details of ROS production upon stimulation with cytokines. To achieve this, ROS generation and cell proliferation upon stimulation with IL-17A, which was identified as the most potent ROS inducer in previous assays, were assessed in ConvR colonic organoid cultures at different timepoints (1 h, 4 h, 18 h, 24 h, 48 h).

Figure 19A demonstrates the time-dependent effects of ROS production upon IL-17A treatment. ROS levels 1 h and 4 h after stimulation are still similar to the control, indicating that the induction is not rapid. After 18 h, the response strongly increases to a >5-fold change, which ultimately peaks at 24 h (6-fold increase) after treatment. After this, the levels start to slowly decline (48 h), supporting the transient nature of ROS. Furthermore, cell proliferation was studied at different timepoints after stimulation (***Figure 19B***). As expected, cell proliferation was not affected by IL-17A treatment at any timepoint, which is reflected in our previous assays.

Altogether, these findings show that the induction of ROS by IL-17A in colonic stem cells is time-dependent, with a maximum response 24 h after treatment, followed by decline after 48

h. The late onset of ROS production suggests a transcriptional response, which should be studied in further experiments.

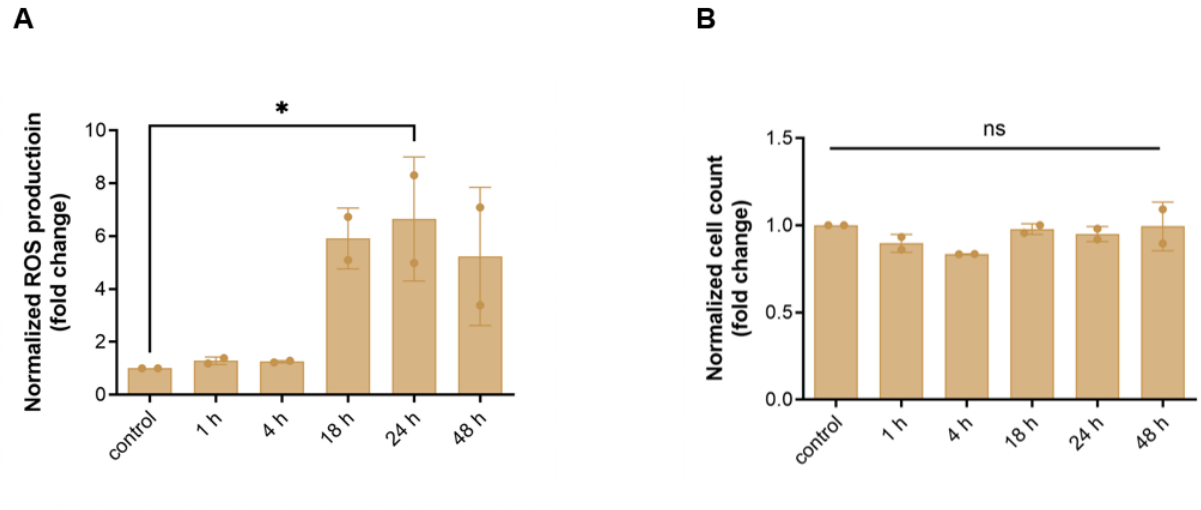

Figure 19 Time-dependent effect of IL-17A stimulation on A) ROS generation and B) cell proliferation. One way ANOVA with Dunnett's multiple comparisons test, * *p<0.05.*

3.3. NGS Wnt-Fc

The proliferative potential of intestinal stem cells is governed by the Wnt signaling pathway. Activation of the pathway induces the activation of target genes required for stem cell homeostasis, and the presence of Wnt factors, in addition to other niche factors, confers adult stem cells their regenerative capacity in *ex vivo* 3D organoid cultures. Hence, Wnt proteins constitute an imperative component of growth media used for the establishment and maintenance of intestinal organoids. Currently, recombinant Wnt3a is commonly used as a Wnt source. However, post-translational palmitoylation of Wnt3a requires addition of serum to stably serve as a medium supplement, introducing undefined experimental conditions (Miao et al., 2020) (Janda et al., 2017). Thus, numerous attempts to develop new Wnt surrogates have been undertaken. Among them, next generation surrogate (NGS) Wnt-Fc has been suggested as a promising none-lipidated water-soluble and receptor-subtype specific alternative to recombinant Wnt3a, supporting organoid growth and maintenance already at low concentrations (Miao et al., 2020). In order to implement NGS Wnt-Fc as a replacement to Wnt3a, the aim of this project was to verify its capacity in supporting organoid culture and to establish a HEK293T cell line displaying high expression of the NGS Wnt-Fc protein, as a means to generate more defined culture conditions for future experiments.

3.3.1. Validation of NGS Wnt-Fc in supporting growth of intestinal organoids

As a first step, the capacity of NGS Wnt-Fc to support proliferation of intestinal organoids was investigated to verify its suitability for downstream experiments. To this end, ConvR colonic organoid cultures were grown in ENR medium supplemented with varying concentrations (0.1 nM-5 nM) of commercially obtained NGS Wnt-Fc. After 48 h, organoid morphology as well as the cell growth rate, i.e. the number of cells grown overtime, were studied using bright-field microscopy and the CellTiterGlo assay respectively.

Concurring with the findings of Miao et al. (2020), organoid growth was supported at all concentrations (***Figure 20***). Notably, while the growth rate was impacted by different concentrations of NGS Wnt-Fc, the stem cell character was successfully maintained in all conditions and differentiation was inhibited. The microscopy data further suggests that the cell growth rate was maximal at supplementation with 5 nM of NGS Wnt-Fc, yielding a similar organoid size as in the control group (50CM). Contrarily, the luminescent data shows that the highest cell growth was determined in cultures supplemented with a 0.5 nM and 2 nM concentration of NGS Wnt-Fc, displaying an approximately 1.4-fold increase compared to the control (50CM). Based on this, a concentration of 0.5 nM was chosen as a standard for medium supplementation in downstream experiments, which is in line with the culture conditions suggested by Miao et al. (2020).

Overall, NGS Wnt-Fc successfully supported organoid growth at different concentrations and maintained stem cell growth in colonic organoid cultures.

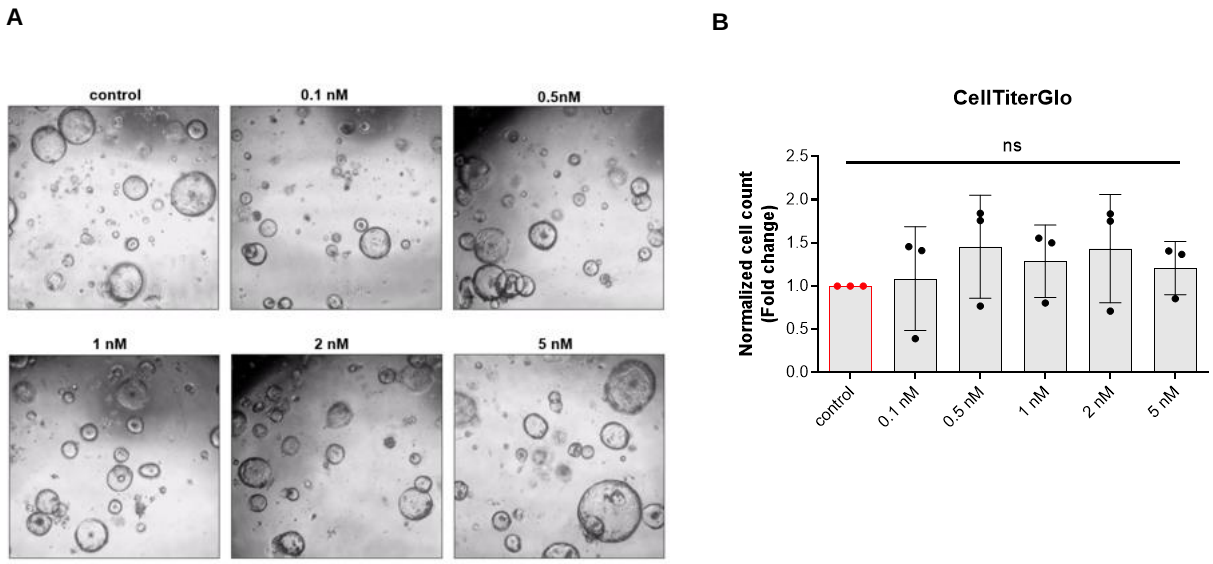

Figure 20 NGS Wnt-Fc supports organoid growth at different concentrations. A) Bright-field microscopy images of ConvR colonic organoid cultures grown in ENR supplemented with varying concentrations of NGS Wnt-Fc (0.1 nM, 0.5 nM, 1 nM, 2 nM, 5 nM). As a control, cells grown in 50CM were analyzed. **B)** Cell count represented as the fold change over the control obtained from the CellTiterGlo assay. Mann-Whitney U test.

3.3.2. Introduction of a Kozak sequence into NGS Wnt-Fc plasmid

After having verified the ability of NGS Wnt-Fc to support the growth and maintenance of colonic organoid cultures, the next aim was to establish a HEK293T cell line displaying high expression of the protein.

To achieve this, a Kozak sequence, i. e. a nucleic acid motif central to the initiation of protein translation in eukaryotes, was introduced into the NGS Wnt-Fc plasmid. Notably, plasmids used in previous attempts to produce NGS Wnt-Fc lacked this motif and displayed low protein production, leading to the hypothesis that introducing the sequence would result in increased expression. As a first step, the nucleic acid motif CACC was inserted at the desired plasmid region, i.e. directly before the translation start codon. This was accomplished by PCR, using primers carrying the respective nucleotides. In order to optimize PCR conditions, gradient PCR using different annealing temperatures was performed (60 °C-70 °C).

***Figure 21*A** shows that DNA amplification was successful at all temperatures. As indicated by the gel bands, the plasmid size was approximately 7 100 bp, which matches the size expected size of the designed plasmid. The strongest band was observed at 66 °C, suggesting that DNA amplification was most optimal at this temperature. As a control, the original NGS Wnt-Fc plasmid was used.

As a next step, the plasmid was purified and digested with the methylation-sensitive restriction enzyme DpnI in order to degrade the methylated parental plasmid DNA. Subsequently, the plasmid was transformed into high plasmid-expressing *E.coli* and the bacterial DNA of the resulting colonies was extracted. To study if the sequence of interest was successfully integrated, the plasmid DNA was analyzed by Sanger sequencing. The sequencing results are shown in ***Figure 21B***.

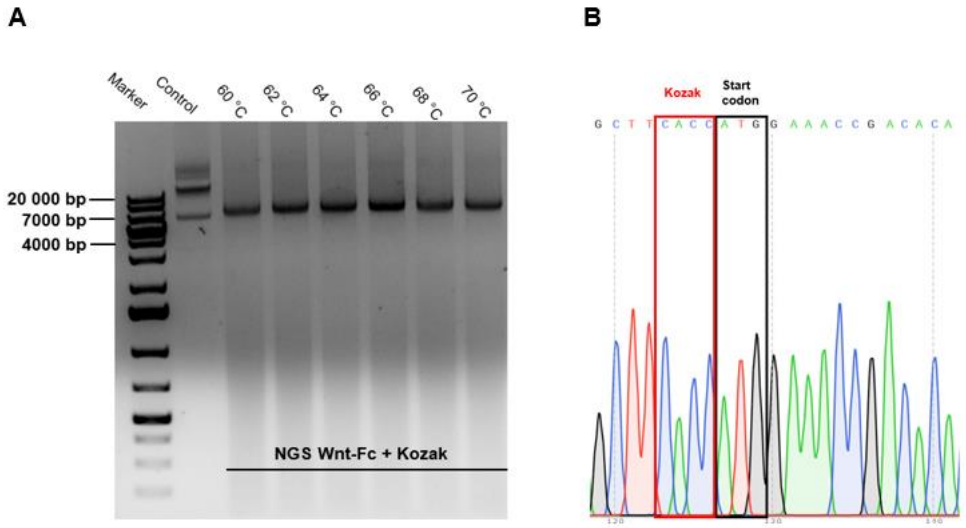

Figure 21 Introduction of the Kozak sequence into the NGS Wnt-Fc plasmid. A) Gradient PCR (60 °C-70 °C) of the NGS Wnt-Fc plasmid using primers carrying the nucleic acid motif CACC. Gel bands were observed at approximately 7 100 bp at all temperatures, with the strongest band at 66 °C. **B)** Sanger sequencing results showing successful integration of the CACC-motif right before the start codon (ATG).

3.3.3. Assessment of NGS Wnt-Fc expression in transiently transfected HEK293T cells

To verify if protein expression is increased in the presence of the Kozak sequence, HEK293T cells were transiently transfected with the mutated NGS Wnt-Fc plasmid and cultured under serum-free conditions in order to prevent interference of gel bands for NGS Wnt-Fc (~64 kDa) and serum-derived BSA (~66 kDa) present in the cell culture medium. To assess protein expression, the culture medium as well as the cell lysate were collected after 24 h and 48 h and analyzed by SDS-PAGE and subsequent western blotting.

The results obtained from immunoblotting show that expression of NGS Wnt-Fc into the medium was increased in HEK293T cells transfected with the plasmid containing the Kozak sequence (***Figure 22***). While no signal was observed for cells transfected with the plasmid lacking the Kozak sequence (-Koz), strong bands were obtained for +Koz cells at 64 kDa after

24 h and 48 h. Furthermore, a second band was observed in +Koz culture medium at approximately 30 kDa, likely resulting from cleavage of the protein between the Wnt-sequence and the Fc-tag due to enterokinase activity. Notably, cell lysates of +Koz cells yielded strong bands at a similar size, indicating that considerable amounts of the protein are present inside the cell. Non-transfected cells were studied as a control.

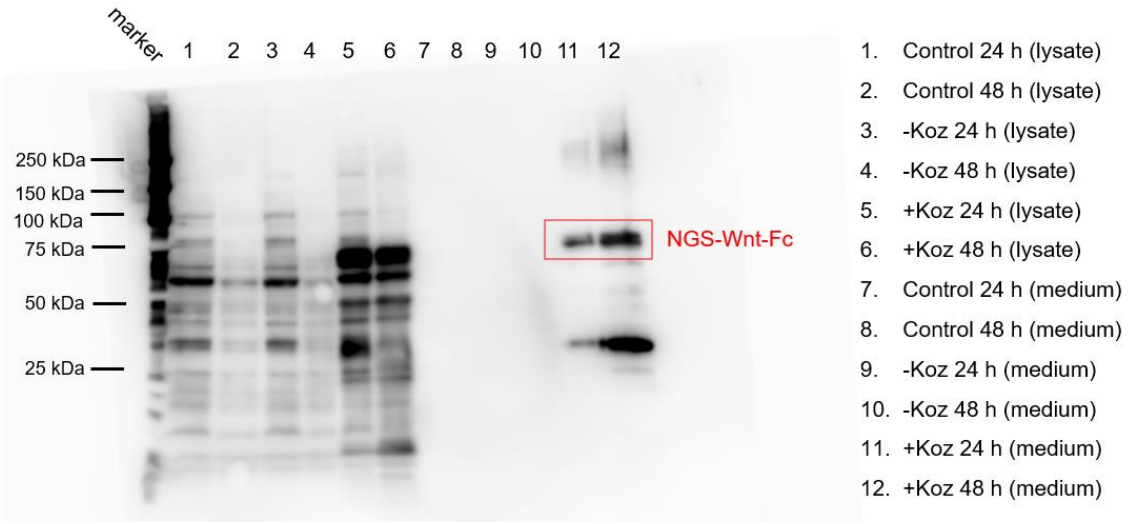

Figure 22 Western blot of transfected HEK293T cells expressing NGS Wnt-Fc. Cell culture media and cell lysates were collected after 24 h and 48 h growth in serum-free medium and analyzed via SDS-PAGE and subsequent western blotting. The primary antibody targeted HIS-tagged proteins (RGSHHHH) and the signal was obtained by chemiluminescent detection of the HRP-conjugated secondary antibody.

Overall, these results demonstrate that the presence of the Kozak sequence strongly enhances the expression of NGS Wnt-Fc in HEK293T cells upon plasmid transfection. Therefore, transient transfection with the mutated NGS Wnt-Fc plasmid presents a promising method of producing the protein in high amounts as a means to use it as a medium supplement for organoid culture.

3.3.4. Establishment of a HEK293T cell line stably expressing NGS Wnt-Fc

Transient transfection leads to short-term alterations of protein expression and its effect is lost over time. In order to achieve continuous expression of NGS Wnt-Fc, the next aim was to stably integrate the target DNA sequence into the HEK293T genomes using the piggyBac transfection system.

To this end, PCR primers were designed to introduce restriction sites for AscI and NotI into the NGS Wnt-Fc plasmid to enable the insertion into a piggyBac vector plasmid. The NGS-WNT plasmid DNA was amplified, purified and, subsequently, digested with AscI and NotI in a sequential digestion to compensate for different buffer requirements. Subsequently, the digested insert was ligated into the vector plasmid and transformed into bacteria. Finally, the

plasmids of selected colonies were purified, the target DNA was amplified by PCR (***Figure 23***) and the sequence was verified by Sanger sequencing.

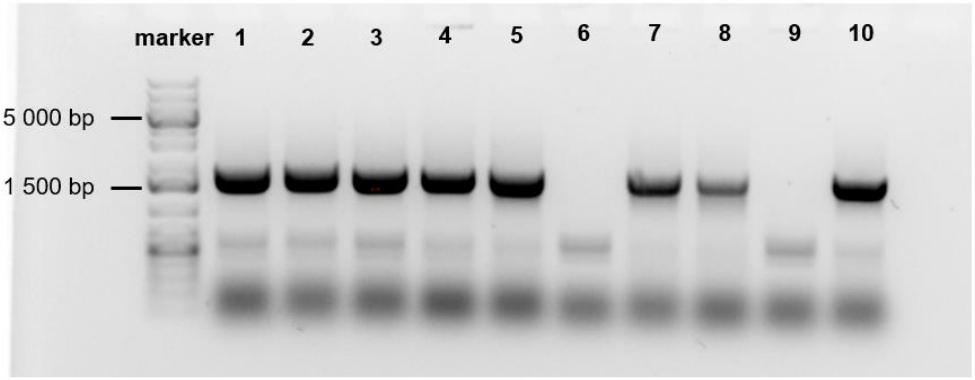

Figure 23 PCR of NGS Wnt-Fc-coding plasmids obtained from bacterial colonies (1-10). The target sequence of interest (1 700 bp) was amplified in all clones, except for 6 and 9.

Subsequently, the plasmid construct was introduced into HEK293T cells by lipofectamine transfection in the presence of the piggyBac transposase-encoding plasmid. The transposase cleaves the vector plasmid at inverted terminal repeats, enabling stable integration of the transposon, carrying the DNA sequence of interest, into the HEK293T cellular genome (S. Zhao et al., 2016). To select for cells that had successfully integrated the target sequence, including a zeocin resistance gene, the cells were challenged with zeocin for 14 days. As controls, cells transfected with only lipofectamine, the transposase-carrying plasmid (pSB cells) or the NGS Wnt-Fc plasmid construct (pXL cells) were used.

As expected, HEK293T cells transfected with the plasmid construct in the presence of the transposase (pXL+psB cells) survived selection, whereas cells transfected with only lipofectamine or only the transposon died within seven days of zeocin treatment, as they lacked the resistance gene. Surprisingly however, cells transfected with the transposon lacking the transposase (pXL) also survived over several weeks of passaging.

Next, protein expression was investigated by analyzing the medium and the cell lysates of pooled HEK293T cells grown in serum-free medium for 48 h. Affinity purification of the His-tag was performed in order to enrich for NGS Wnt-Fc in the cell culture medium. Subsequently, protein production was studied in the culture media and cell lysates using SDS-PAGE and western blotting.

The results for SDS-PAGE and western blotting are depicted in ***Figure 24***. Unexpectedly, SDS-PAGE analysis revealed bands at ~64 kDa for the non-enriched and the bead-depleted fraction of pXL+pSB culture medium as well as in the non-enriched fraction of pXL culture medium. However, no bands were detected in the enriched conditions. Contrarily, bands at 64

kDa and 20 kDa were detected in enriched fractions by western blotting, indicating that the affinity purification was successful. Notably, no bands were observed in pXL fractions.

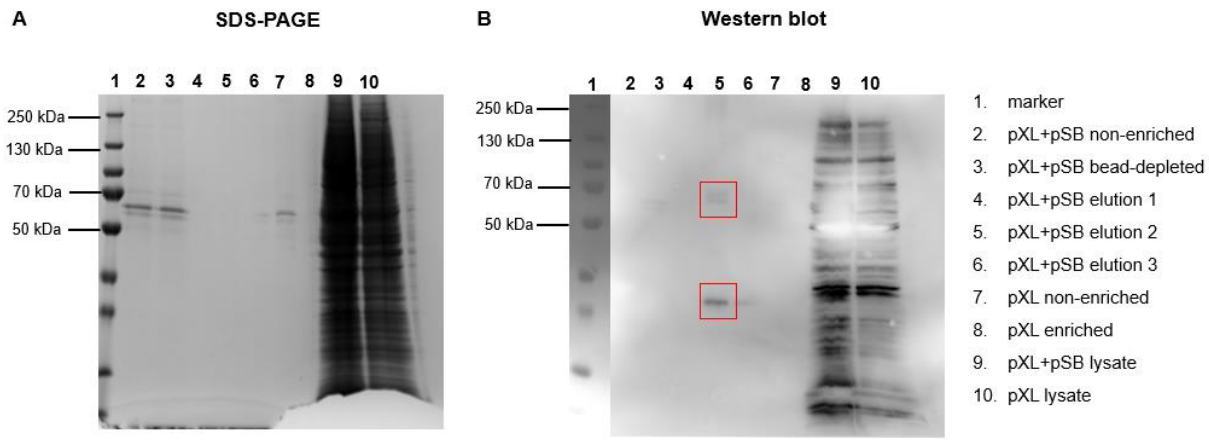

Figure 24 Detection of NGS Wnt-Fc expression in stably transfected HEK293T cells. **A)** SDS-PAGE and **B)** western blot results of medium samples, including their elution fractions, and cell lysates of pXL+pSB and pXL cells. HIS-tagged proteins (RGSHHHH) were targeted by the primary antibody and the signal was obtained by chemiluminescent detection of the HRP-conjugated secondary antibody.

A varying number of DNA copies are inserted into each genome when applying the piggyBac system. Due to this, cells display differences in protein expression depending on the number of integrated gene constructs. To identify cells showing high protein production, single cell clonal selection was performed and expression of NGS Wnt-Fc was again investigated by SDS-PAGE and western blotting after 48 h in serum-free culture conditions.

As shown in ***Figure 25***, protein expression in single clones was generally low. Nevertheless, a weak band at 64 kDa was identified for clone 12. In order to verify whether the identified band corresponds to NGS Wnt-Fc or whether it resulted from BSA remnants (66 kDa) present in the medium, mass spectrometry was performed ***Table 11***. As the data reveals, NGS Wnt-Fc is present in the gel band, albeit in small amounts. Notably, BSA represented the major component in the sample. This is in line with the observation made in for non-enriched fractions in SDS-PAGE experiments, where the bands in the non-enriched fractions correspond to BSA remnants still present in serum-free conditions. Therefore, additional washing steps were introduced before switching to serum-free conditions.

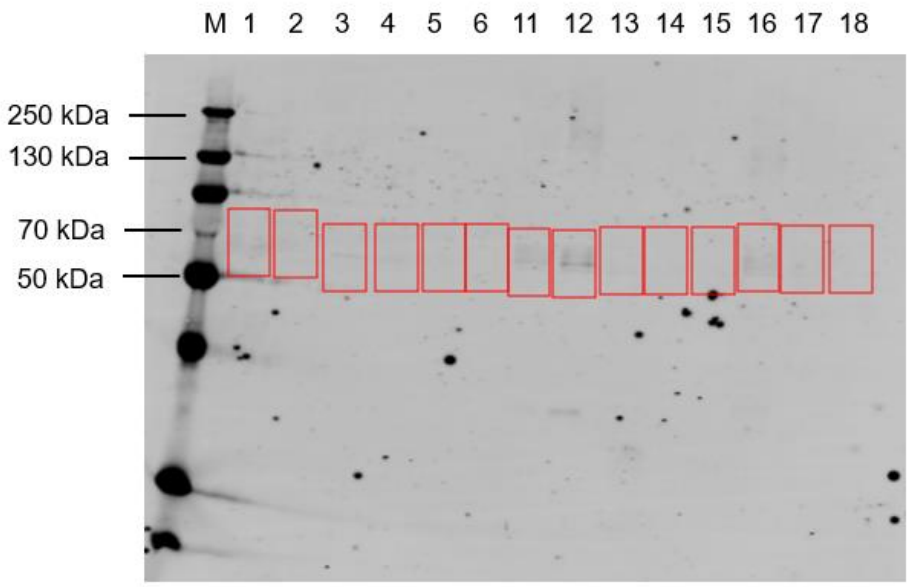

Figure 25 Western Blot of HEK293T single cell clones. Medium samples were collected after 48 h and analyzed without purification of NGS Wnt-Fc. The primary antibody target were HIS-tagged proteins (RGSHHHH). The signal was obtained by fluorescent detection of the Alexa Fluor-labelled secondary antibody.

While serum-free conditions are required for the downstream analysis of NGS Wnt-Fc expression, HEK293T display higher cell growth and protein expression in IMDM culture medium supplemented with serum. To eradicate this as a possible cause for reduced protein expression, cells were sequentially adapted to Freestyle293 medium, reported to show improved growth despite not containing serum. Based on the results obtained in ***Figure 25***, clone 12 and clone 3 were chosen as candidates for testing NGS Wnt-Fc expression in optimized growth conditions. The clones were grown in Freestyle293 for 48 h and the medium and the cell lysates were analyzed via western blotting. Notably, cells grown in Freestyle293 medium displayed increased viability compared to culture in SF IMDM. However, the preliminary results obtained were similar to SF-IMDM, with NGS Wnt-Fc expression was not being increased in any condition.

To conclude, NGS Wnt-Fc reliably supports organoid maintenance and proliferation in ConvR colonic organoids, presenting a promising alternative to serum-stabilized Wnt3a. Furthermore, transient transfection of HEK293T cells with a mutated NGS Wnt-Fc plasmid containing a Kozak sequence achieved high levels of protein expression, presenting an option to produce and purify the protein within the facility. In addition, preliminary data obtained from western blotting suggests that stable integration of the NGS Wnt-Fc-coding DNA sequence into the HEK293T cellular genome might result in sustainable production of the protein. However, this needs further investigations, especially regarding the optimization of culture conditions in order to exclude possible signal contamination caused by BSA. Lastly, further research should be done on the identification of single clones displaying higher protein expression.

Gene name	Protein name	Species	Peptides identified
ALB	Albumin	*Bos taurus*	23
KRT1	Keratin, type II cytoskeletal 1	*Homo sapiens*	29
	Trypsin	*Sus scrofa*	4
HSPA1A	Heat-shock 70 kDa protein 1A	*Homo sapiens*	23
KRT9	Keratin, type I cytoskeletal 9	*Homo sapiens*	22
NGSWNT	NGS WNT	*Homo sapiens*	6

Table 11 Mass spectrometry results showing relative protein abundance in medium collected from transfected HEK293 cells.

4. Discussion

The intestinal epithelium lining the gastrointestinal tract presents the primary point of interaction of the host with the outside world (Van Der Post et al., 2021). ISCs, residing at the base of the intestinal crypt, confer the intestinal epithelium its regenerative potential and play a vital role in balancing self-renewal and differentiation, thereby contributing to the maintenance of gut homeostasis (Beumer & Clevers, 2021). In the colon, proliferating stem cells have been shown to display high activity of the enzyme NOX1, which promotes cell growth via the ROS-induced activation of EGFR (Van Der Post et al., 2021). ISC function and development are vastly shaped by external cues, including cytokines secreted from gut-resident immune cells, that are produced in response to a wide range of stimuli. However, exact details of the impact of the complex network of cytokines on ISC function are not yet fully elucidated (Pavlidis et al., 2022). The development of intestinal organoids has been pivotal for gastrointestinal research. Due to their capacity to recapitulate the 3D-architecture of the organ of origin, organoids have enabled great advances in basic research, disease modelling, drug discovery and personalized medicine (Z. Zhao et al., 2022). Currently, stem-cell maintaining niche factors used in organoid culture, including Wnt, R-spondin and noggin, are administered via conditioned medium (Miyoshi & Stappenbeck, 2013). However, the widely used recombinant Wnt-version Wnt3a requires the addition of serum for lipid-stabilization, introducing undefined experimental parameters (Tüysüz et al., 2017). Hence, there is a search for new Wnt surrogates with the goal of optimizing culture conditions (Miao et al., 2020). Here, we studied the impact of a library of selected cytokines on colonic stem cells as a means to gain insight into their potential implications in differentiation and self-renewal via the production of ROS. Furthermore, we aimed to establish a NGS Wnt-Fc producing cell line with the goal of optimizing the culture of intestinal organoids.

Our research approach was based on the observation that intestinal homeostasis is altered in response to NOX1-derived ROS (Van Der Post et al., 2021). Despite their vital role in cellular signaling, physiological functions of ROS are often confined to their involvement in antimicrobial defense mechanisms and pathogen killing. Although great advances to shed light onto the role of ROS-mediated signaling in the intestine have been made (Hong et al., 2024), their detailed role in controlling proliferation and differentiation remains elusive. In order to contribute to solving this question, we established colonic organoid cultures from different mouse models in order to investigate changes in cell proliferation, differentiation state and NOX1-mediated ROS generation. Selected cytokines were administered in 50CM or ENR medium 24 h or 48 h after seeding. Readouts were performed 48 h or 72 h after treatment via fluorescence- and luminescence-based plate-reader assays as well as mass spectrometry.

The results of our work have identified IL-13 and IL-22 as drivers of goblet cell differentiation in colonic stem cells. Our plate-reader assay analysis showed an increase of mCherry-signal for organoid cultures stimulated with these cytokines, corresponding to an elevated expression of MUC2 (***Figure 9A***). In further support of this, mass spectrometry analysis (***Figure 10***) revealed a significant upregulation of MUC2, FCGBP and CLCA1 protein levels upon IL-13 stimulation, while this upregulation was not observed for IL-22. These findings are in line with observations made by Lindholm et al. (2022), who reported quantitative changes in goblet cell numbers in response to IL-13 stimulation, supported by high MUC2 expression levels, while IL-22 was linked to qualitative changes in goblet cell state, indicated by elevated levels of the goblet cell marker RELMβ and low MUC2 levels. Interestingly, IL-13 induced goblet cell differentiation even under stem-cell maintaining conditions, suggesting a powerful capacity to override regenerative cues at the intestinal crypt (***Figure 9C***). A possible mechanism for this is IL-13's ability to induce Bmp-signaling (Lindholm et al., 2022), shifting the balance from a proliferation-promoting environment to a differentiation-inducing one. In addition, differentiating effects were reflected in the cell number for IL-13 and IL-22 (***Figure 9B***), where a decrease in proliferation correlates with an increased differentiation state. High mCherry signals were also observed for IL-13 and IL-22 in fluorescence microscopy (***Figure 8***), further corroborating these findings. However, the fluorescent images also display elevated signals for TNF-α and IL-17A, despite no differentiating effects being observed in other assays. This discrepancy is likely due to the low seeding number of cells in this experimental run, impacting its outcome. Hence, this experiment should be repeated in order to fully capture the effects of cytokine stimulation on differentiation. Moreover, our data does not fully uncover the implications of IFN-γ in goblet cell differentiation. The plate-reader data suggests a potential involvement in promoting goblet cell differentiation. However, based on the impairment of organoid growth and morphology upon treatment, we hypothesize that these signals occur due to autofluorescence caused by IFN-γ-induced cell death. IFN-γ signaling has been associated with the regulation of mucus secretion and goblet cell function, especially upon infection with *Salmonella* Typhimurium (Songhet et al., 2011). However, previous studies have also described a role of IFN-γ in the induction of stem cell death in the inflamed intestine (Kretzschmar & Clevers, 2019). To investigate this further, we studied cytokine-induced cytotoxicity (**Figure *11***) and found only slightly elevated levels upon IFN-γ stimulation. Importantly, cytotoxicity was assessed in 50CM, i.e. under stem cell-maintaining conditions, while impaired growth was observed under differentiating conditions. Hence, we propose a cytotoxic effect for IFN-γ under differentiating conditions at the concentration used for our experiments, while it does not induce cell damage at the stem cell compartment. However, this should be verified by determining cytotoxicity under differentiation conditions. Lastly, TNF-α,

IL-17A and IL-10 did not show significant impacts on goblet cell differentiation, concurring with the current literature.

Earlier work has shown implications of IL-17 (Kumar et al., 2016) and IL-22 (Leung & Loke, 2013) in controlling intestinal homeostasis as well as the mechanisms of ROS generation in skin inflammation and neurodegenerative disease (Fu et al., 2022) (Cho et al., 2012). To expand on this, we aimed to establish a link of ROS generation and gut homeostasis via the analysis of expression levels of NOX1 upon cytokine stimulation. Indeed, we identified T_h17-derived IL-17A and IL-22 as potent drivers of ROS generation in GF as well as ConvR colonic organoids in luminescence-based plate-reader assays (***Figure 12***). In addition, ROS production was found to be strongly reduced in response to IL-13 stimulation, indicating strong antioxidant effects in the colon. Furthermore, IFN-γ stimulation yielded increased ROS levels in GF, but not in ConvR mice, which suggests potential immune modulatory effects of the microbiota on the IFN-γ response upon conventionalization. The enzymatic sources of cytokine-induced ROS were additionally analyzed by mass spectrometry (***Figure 14***). NOX1 expression levels were highly upregulated upon IL-17A stimulation, whereas downregulation was observed for IL-13 and IL-22. All three cytokines showed an upregulation of differentiation-associated DUOX2. Furthermore, NOS2 expression was highly increased upon IFN-γ and IL-22 treatment and decreased by IL-13. Moreover, expression of the proliferation markers MKI67, PCNA and CDK1 was reduced in response to IL-13 and IL-17A, with PCNA being additionally decreased upon IL-22 stimulation. Overall, this suggests inhibitory effects on cell proliferation for these cytokines. Our data further shows the time-dependent effect of IL-17A-mediated ROS expression, with induction reaching a maximum after 24 h of stimulation, while slowly starting to decrease after 48 h (***Figure 19***). The relatively late onset of production might indicate transcriptional responses, however, this should be studied in future experiments. The plate-reader results further show concentration-dependent effects upon treatment with TNF-α and IFN-γ, displaying an increased and decreased ROS expression with increasing concentration respectively (***Figure 17***). This dose-dependent effect was not reflected in the cell numbers (***Figure 18***), which does not necessarily contradict the involvement of NOX1-mediated ROS expression on proliferation, as TNF-α and IFN-γ were shown to not act via NOX1 (***Figure 14***). Importantly, a large body of evidence points to implications of TNF-α in the maintenance of intestinal integrity by controlling important cell fate decisions, including cell proliferation as well as cell death and survival, via the induction of signaling cascades (Leppkes et al., 2014). Notably, treatment strategies targeting TNF-α have been among the most successful clinical approaches for treating IBD. However, the impacts observed for TNF-α within this study have been limited. A possible explanation for this is that the standard concentration used for stimulation (10 ng/mL) is too low to induce observable changes, which is supported by our results for the concentration series, showing effects on ROS expression at

higher concentrations. Another possibility would be that TNF-α exerts its effects mainly synergistically, i. e. when acting together with other cytokines, however, this is less likely based on previous studies (Xing et al., 2023). Lastly, a potential error in the TNF-α source used in our experiments might lead to lower activity, which should be verified in future experiments. Finally, IL-10 did not show any effect on proliferation or ROS generation.

To conclude, our results suggest a role for IL-13 and IL-22 in protective mechanisms in the gastrointestinal tract through increased mucus production upon induction of goblet cell expression. It has been shown that both IL-13 and IL-22 are often involved in the clearance of helminth infections (Giuffrida et al., 2019) (Keir et al., 2020), where an increase in goblet cell production helps with the weep and sweep mechanisms for pathogen clearance (Lindholm et al., 2022). Interestingly, IL-13 has also been implicated with the impairment of mucosal permeability and damage of the epithelial barrier in UC patients (Tatiya-aphiradee et al., 2018), implicating a role in disease progression. Hence, there is a need to uncover the pleiotropic functions that IL-13 exerts in the intestine in order to gain more insight into its role in protection and pathogenesis. Moreover, we have identified IL-17A and IL-22 as important drivers of ROS generation in the colon, whereas only IL17A-mediated ROS expression can be tied to NOX1 activity. Interestingly, IL-17A-derived ROS was correlated with a decrease in cell proliferation, which is unexpected based on the notion that NOX1 is a marker for proliferating colonic stem cells (Van Der Post et al., 2021). It is possible that IL-17A induces ROS at supraphysiological levels, thereby potentially causing cell damage leading to the decrease in cell growth. However, this has to be studied in future experiments. Lastly, we found NOX1-mediated ROS expression and cell proliferation to be highly reduced in IL-13-treated organoid cultures, further underlining its differentiating effects. Overall, this is in line with previous observations showing that NOX1 expression is confined to the stem cell compartment and is not found in terminally differentiated cells (Van Der Post et al., 2021).

As a second part of the project, we have investigated the capacity of NGS Wnt-Fc to replace Wnt3a in organoid culture and aimed to establish a cell line as a means to produce the protein within our facility. Our choice was based on findings by Miao et al. (2020), who described a promising ability of NGS Wnt-Fc to support organoid expansion and long-term maintenance, while at the same time displaying improved solubility in water. Notably, previous efforts within the department to produce NGS Wnt-Fc using an expression cell line yielded low protein production levels. Based on this observation, we hypothesized that introducing a Kozak sequence into the NGS Wnt-Fc plasmid would enhance protein expression upon transfection.

In accordance with results from Miao et al. (2020), we have found that NGS Wnt-Fc is capable to support organoid growth, while at the same time maintaining stem cell function (***Figure 20***). After having verified this, we inserted the nucleic acid motif CACC (Kozak sequence) into the

original plasmid using PCR and, subsequently, investigated protein production upon transient transfection into HEK293T cells. Indeed, our results show that production of NGS Wnt-Fc was enhanced in medium collected after 24 h and 48 h, supporting our starting hypothesis. Based on this, we next aimed to stably integrate the NGS Wnt-Fc target sequence into the HEK293T cellular genome using the PiggyBac system in order to yield stable expression of the protein. Our sequencing results show that the target sequence was successfully integrated into the PiggyBac vector. Furthermore, zeocin selection further underlined the successful uptake of the resistance gene included in the target sequence. As the PiggyBac system is based on integration of the target at random sites within the genome, expression levels of the protein vary within individual cells (S. Zhao et al., 2016). Due to this reason, we established a library of single clones and analyzed their expression levels via SDS-PAGE and western blotting. Our analysis was greatly complicated by the fact that NGS Wnt-Fc has a similar molecular weight to serum-derived BSA, making a distinguishment difficult. Finally, we identified via mass spectrometry that NGS Wnt-Fc was indeed produced by our cell line, however, only in small amounts, with the main signal resulting from residual BSA (***Table 11***). One possibility for this is that secretion of the NGS Wnt-Fc protein is impaired, retaining the protein within the cell. This is supported by the observation that cell lysates showed similar bands to culture medium (***Figure 22***). Another possible explanation is that single cell clones did not produce individual cells from which the clones were started, but rather an assembly of 2-3 cells that display different expression levels. Based on this, we hypothesize that HEK293T cells displaying high protein expression might show a reduced proliferation rate due to cellular stress responses, leading to selective mechanisms in which low-expressing and fast-dividing cells override the high-expressing cells. Hence, we recommend repeating the single cell cloning in order to rule out possible error having occurred. Furthermore, we observed that pXL cells, which were transfected with PiggyBac vector in absence of the transposase, also survived zeocin selection, despite them not having the plasmid stably integrated. A possible reason might be contamination with pXL+pSB cells, however, this is unlikely because western blot analysis of pXL cells yielded different band patterns than in pXL+pSB cells.

Possible limitations of this study include the inherent heterogeneity of organoids, which can impact experimental reproducibility. Despite their potential to recapitulate structure and function of the organ of interest, making them an invaluable research tool, they do not fully capture the full complexity of their *in vivo* counterpart. Furthermore, the results of plate-reader assays are highly impacted by the seeding number of cells, for which the determination is less straight-forward in organoid cultures than it is in immortalized cell lines. Hence, it is of great importance to establish methods to standardize seeding in order to minimize experimental variability. Moreover, an identification of drivers of proliferation in our experimental setup is more difficult than the identification of inhibitors, as the control conditions are already under

optimal growth conditions in 50CM control used. Hence, we advise to generate growth conditions in which cell growth is slowed down in order to be able to identify proliferation-promoting factors.

In future projects, we aim to connect cytokine-mediated changes in ISC function and development with responses mediated by microbiome-derived metabolites in order to extend our knowledge of the interactions of the microbiome with the immune system. Furthermore, we will perform co-culturing experiments of colonic stem cells with immune cells in order to identify the immune cells responsible for the observed response. Lastly, we aim to study different combinations of cytokines on ISCs to get a more extensive and representative insight into the interplay of cytokines at the intestinal crypt.

5. Bibliography

Beumer, J., & Clevers, H. (2021). Cell fate specification and differentiation in the adult mammalian intestine. *Nature Reviews Molecular Cell Biology*, *22*(1), 39–53. https://doi.org/10.1038/s41580-020-0278-0

Biton, M., Haber, A. L., Rogel, N., Burgin, G., Beyaz, S., Schnell, A., Ashenberg, O., Su, C.-W., Smillie, C., Shekhar, K., Chen, Z., Wu, C., Ordovas-Montanes, J., Alvarez, D., Herbst, R. H., Zhang, M., Tirosh, I., Dionne, D., Nguyen, L. T., … Xavier, R. J. (2018). T Helper Cell Cytokines Modulate Intestinal Stem Cell Renewal and Differentiation. *Cell*, *175*(5), 1307-1320.e22. https://doi.org/10.1016/j.cell.2018.10.008

Bjerknes, M., & Cheng, H. (1999). Clonal analysis of mouse intestinal epithelial progenitors. *Gastroenterology*, *116*(1), 7–14. https://doi.org/10.1016/S0016-5085(99)70222-2

Cheng, H., & Leblond, C. P. (1974). Origin, differentiation and renewal of the four main epithelial cell types in the mouse small intestine V. Unitarian theory of the origin of the four epithelial cell types. *American Journal of Anatomy*, *141*(4), 537–561. https://doi.org/10.1002/aja.1001410407

Cho, K.-A., Suh, J. W., Lee, K. H., Kang, J. L., & Woo, S.-Y. (2012). IL-17 and IL-22 enhance skin inflammation by stimulating the secretion of IL-1β by keratinocytes via the ROS-NLRP3-caspase-1 pathway. *International Immunology*, *24*(3), 147–158. https://doi.org/10.1093/intimm/dxr110

Friedrich, M., Pohin, M., & Powrie, F. (2019). Cytokine Networks in the Pathophysiology of Inflammatory Bowel Disease. *Immunity*, *50*(4), 992–1006. https://doi.org/10.1016/j.immuni.2019.03.017

Fu, J., Huang, Y., Bao, T., Liu, C., Liu, X., & Chen, X. (2022). The role of Th17 cells/IL-17A in AD, PD, ALS and the strategic therapy targeting on IL-17A. *Journal of Neuroinflammation*, *19*(1), 98. https://doi.org/10.1186/s12974-022-02446-6

Gehart, H., & Clevers, H. (2019). Tales from the crypt: New insights into intestinal stem cells. *Nature Reviews Gastroenterology & Hepatology*, *16*(1), 19–34. https://doi.org/10.1038/s41575-018-0081-y

Giuffrida, P., Caprioli, F., Facciotti, F., & Di Sabatino, A. (2019). The role of interleukin-13 in chronic inflammatory intestinal disorders. *Autoimmunity Reviews*, *18*(5), 549–555. https://doi.org/10.1016/j.autrev.2019.03.012

Gustafsson, J. K., & Johansson, M. E. V. (2022). The role of goblet cells and mucus in intestinal homeostasis. *Nature Reviews Gastroenterology & Hepatology*, *19*(12), 785–803. https://doi.org/10.1038/s41575-022-00675-x

Hong, Y., Boiti, A., Vallone, D., & Foulkes, N. S. (2024). Reactive Oxygen Species Signaling and Oxidative Stress: Transcriptional Regulation and Evolution. *Antioxidants*, *13*(3), 312. https://doi.org/10.3390/antiox13030312

Hou, Q., Huang, J., Ayansola, H., Masatoshi, H., & Zhang, B. (2021). Intestinal Stem Cells and Immune Cell Relationships: Potential Therapeutic Targets for Inflammatory Bowel Diseases. *Frontiers in Immunology*, *11*, 623691. https://doi.org/10.3389/fimmu.2020.623691

Hsu, N.-Y., Nayar, S., Gettler, K., Talware, S., Giri, M., Alter, I., Argmann, C., Sabic, K., Thin, T. H., Ko, H.-B. M., Werner, R., Tastad, C., Stappenbeck, T., Azabdaftari, A., Uhlig, H. H., Chuang, L.-S., & Cho, J. H. (2023). NOX1 is essential for TNFα-induced intestinal epithelial ROS secretion and inhibits M cell signatures. *Gut*, *72*(4), 654–662. https://doi.org/10.1136/gutjnl-2021-326305

Janda, C. Y., Dang, L. T., You, C., Chang, J., De Lau, W., Zhong, Z. A., Yan, K. S., Marecic, O., Siepe, D., Li, X., Moody, J. D., Williams, B. O., Clevers, H., Piehler, J., Baker, D., Kuo, C. J., & Garcia, K. C. (2017). Surrogate Wnt agonists that phenocopy canonical Wnt and β-catenin signalling. *Nature*, *545*(7653), 234–237. https://doi.org/10.1038/nature22306

Keir, M. E., Yi, T., Lu, T. T., & Ghilardi, N. (2020). The role of IL-22 in intestinal health and disease. *Journal of Experimental Medicine*, *217*(3), e20192195. https://doi.org/10.1084/jem.20192195

Kretzschmar, K., & Clevers, H. (2019). IFN-γ: The T cell's license to kill stem cells in the inflamed intestine. *Science Immunology*, *4*(42), eaaz6821. https://doi.org/10.1126/sciimmunol.aaz6821

Kumar, P., Monin, L., Castillo, P., Elsegeiny, W., Horne, W., Eddens, T., Vikram, A., Good, M., Schoenborn, A. A., Bibby, K., Montelaro, R. C., Metzger, D. W., Gulati, A. S., & Kolls, J. K. (2016). Intestinal Interleukin-17 Receptor Signaling Mediates Reciprocal Control of the Gut Microbiota and Autoimmune Inflammation. *Immunity*, *44*(3), 659–671. https://doi.org/10.1016/j.immuni.2016.02.007

Leppkes, M., Roulis, M., Neurath, M. F., Kollias, G., & Becker, C. (2014). Pleiotropic functions of TNF-α in the regulation of the intestinal epithelial response to inflammation. *International Immunology*, *26*(9), 509–515. https://doi.org/10.1093/intimm/dxu051

Leung, J. M., & Loke, P. (2013). A role for IL-22 in the relationship between intestinal helminths, gut microbiota and mucosal immunity. *International Journal for Parasitology*, *43*(3–4), 253–257. https://doi.org/10.1016/j.ijpara.2012.10.015

Lin, X., Gaudino, S. J., Jang, K. K., Bahadur, T., Singh, A., Banerjee, A., Beaupre, M., Chu, T., Wong, H. T., Kim, C.-K., Kempen, C., Axelrad, J., Huang, H., Khalid, S., Shah, V., Eskiocak, O., Parks, O. B., Berisha, A., McAleer, J. P., … Kumar, P. (2022). IL-17RA-signaling in Lgr5+ intestinal stem cells induces expression of transcription factor

ATOH1 to promote secretory cell lineage commitment. *Immunity*, *55*(2), 237-253.e8. https://doi.org/10.1016/j.immuni.2021.12.016

Lindholm, H. T., Parmar, N., Drurey, C., Campillo Poveda, M., Vornewald, P. M., Ostrop, J., Díez-Sanchez, A., Maizels, R. M., & Oudhoff, M. J. (2022). BMP signaling in the intestinal epithelium drives a critical feedback loop to restrain IL-13–driven tuft cell hyperplasia. *Science Immunology*, *7*(71), eabl6543. https://doi.org/10.1126/sciimmunol.abl6543

Mannon, P., & Reinisch, W. (2012). Interleukin 13 and its role in gut defence and inflammation. *Gut*, *61*(12), 1765–1773. https://doi.org/10.1136/gutjnl-2012-303461

McCarthy, H., & Keely, S. (2023). Re-evaluating the Role of Deep Crypt Secretory Cells in Intestinal Homeostasis. *Cellular and Molecular Gastroenterology and Hepatology*, *15*(4), 1020–1021. https://doi.org/10.1016/j.jcmgh.2023.01.005

Miao, Y., Ha, A., De Lau, W., Yuki, K., Santos, A. J. M., You, C., Geurts, M. H., Puschhof, J., Pleguezuelos-Manzano, C., Peng, W. C., Senlice, R., Piani, C., Buikema, J. W., Gbenedio, O. M., Vallon, M., Yuan, J., De Haan, S., Hemrika, W., Rösch, K., … Garcia, K. C. (2020). Next-Generation Surrogate Wnts Support Organoid Growth and Deconvolute Frizzled Pleiotropy In Vivo. *Cell Stem Cell*, *27*(5), 840-851.e6. https://doi.org/10.1016/j.stem.2020.07.020

Mihara, E., Hirai, H., Yamamoto, H., Tamura-Kawakami, K., Matano, M., Kikuchi, A., Sato, T., & Takagi, J. (2016). Active and water-soluble form of lipidated Wnt protein is maintained by a serum glycoprotein afamin/α-albumin. *eLife*, *5*, e11621. https://doi.org/10.7554/eLife.11621

Miyoshi, H., & Stappenbeck, T. S. (2013). In vitro expansion and genetic modification of gastrointestinal stem cells in spheroid culture. *Nature Protocols*, *8*(12), 2471–2482. https://doi.org/10.1038/nprot.2013.153

Naik, S., Larsen, S. B., Cowley, C. J., & Fuchs, E. (2018). Two to Tango: Dialog between Immunity and Stem Cells in Health and Disease. *Cell*, *175*(4), 908–920. https://doi.org/10.1016/j.cell.2018.08.071

Neurath, M. F. (2014). Cytokines in inflammatory bowel disease. *Nature Reviews Immunology*, *14*(5), 329–342. https://doi.org/10.1038/nri3661

Pavlidis, P., Tsakmaki, A., Treveil, A., Li, K., Cozzetto, D., Yang, F., Niazi, U., Hayee, B. H., Saqi, M., Friedman, J., Korcsmaros, T., Bewick, G., & Powell, N. (2022). Cytokine responsive networks in human colonic epithelial organoids unveil a molecular classification of inflammatory bowel disease. *Cell Reports*, *40*(13), 111439. https://doi.org/10.1016/j.celrep.2022.111439

Pérez, S., Taléns-Visconti, R., Rius-Pérez, S., Finamor, I., & Sastre, J. (2017). Redox signaling in the gastrointestinal tract. *Free Radical Biology and Medicine*, *104*, 75–103. https://doi.org/10.1016/j.freeradbiomed.2016.12.048

Qi, Z., & Chen, Y.-G. (2015). Regulation of intestinal stem cell fate specification. *Science China Life Sciences*, *58*(6), 570–578. https://doi.org/10.1007/s11427-015-4859-7

Ramos, G. P., & Papadakis, K. A. (2019). Mechanisms of Disease: Inflammatory Bowel Diseases. *Mayo Clinic Proceedings*, *94*(1), 155–165. https://doi.org/10.1016/j.mayocp.2018.09.013

Saeid Seyedian, S., Alimentary Tract Research Center, Ahvaz Jundishapur University of Medical Science, Ahvaz, Iran, Nokhostin, F., Faculty of Medicine, Ahvaz Jundishapur University of Medical Sciences, Ahvaz, Iran, Forogh Nokhostin, Assistant Professor of Internal Medicine, Faculty of Medicine, Ahvaz Jundishapur University of Medical Sciences, Ahvaz, Iran, Phone: +989163723286, E-mail: Forogh_Nokhostin@yahoo.com, Dargahi Malamir, M., & Faculty of Medicine, Medical doctor of Internal Medicine, Ahvaz Jundishapur University of Medical Sciences, Ahvaz, Iran. (2019). A review of the diagnosis, prevention, and treatment methods of inflammatory bowel disease. *Journal of Medicine and Life*, *12*(2), 113–122. https://doi.org/10.25122/jml-2018-0075

Sahoo, D. K., Heilmann, R. M., Paital, B., Patel, A., Yadav, V. K., Wong, D., & Jergens, A. E. (2023). Oxidative stress, hormones, and effects of natural antioxidants on intestinal inflammation in inflammatory bowel disease. *Frontiers in Endocrinology*, *14*, 1217165. https://doi.org/10.3389/fendo.2023.1217165

Sartor, R. B. (2006). Mechanisms of Disease: Pathogenesis of Crohn's disease and ulcerative colitis. *Nature Clinical Practice Gastroenterology & Hepatology*, *3*(7), 390–407. https://doi.org/10.1038/ncpgasthep0528

Sato, T., Vries, R. G., Snippert, H. J., Van De Wetering, M., Barker, N., Stange, D. E., Van Es, J. H., Abo, A., Kujala, P., Peters, P. J., & Clevers, H. (2009). Single Lgr5 stem cells build crypt-villus structures in vitro without a mesenchymal niche. *Nature*, *459*(7244), 262–265. https://doi.org/10.1038/nature07935

Schreurs, R. R. C. E., Baumdick, M. E., Sagebiel, A. F., Kaufmann, M., Mokry, M., Klarenbeek, P. L., Schaltenberg, N., Steinert, F. L., Van Rijn, J. M., Drewniak, A., The, S.-M. M. L., Bakx, R., Derikx, J. P. M., De Vries, N., Corpeleijn, W. E., Pals, S. T., Gagliani, N., Friese, M. A., Middendorp, S., … Bunders, M. J. (2019). Human Fetal TNF-α-Cytokine-Producing CD4+ Effector Memory T Cells Promote Intestinal Development and Mediate Inflammation Early in Life. *Immunity*, *50*(2), 462-476.e8. https://doi.org/10.1016/j.immuni.2018.12.010

Sies, H., Belousov, V. V., Chandel, N. S., Davies, M. J., Jones, D. P., Mann, G. E., Murphy, M. P., Yamamoto, M., & Winterbourn, C. (2022). Defining roles of specific reactive oxygen species (ROS) in cell biology and physiology. *Nature Reviews Molecular Cell Biology*, *23*(7), 499–515. https://doi.org/10.1038/s41580-022-00456-z

Songhet, P., Barthel, M., Stecher, B., Müller, A. J., Kremer, M., Hansson, G. C., & Hardt, W.-D. (2011). Stromal IFN-γR-Signaling Modulates Goblet Cell Function During Salmonella Typhimurium Infection. *PLoS ONE*, *6*(7), e22459. https://doi.org/10.1371/journal.pone.0022459

Suriano, F., Nyström, E. E. L., Sergi, D., & Gustafsson, J. K. (2022). Diet, microbiota, and the mucus layer: The guardians of our health. *Frontiers in Immunology*, *13*, 953196. https://doi.org/10.3389/fimmu.2022.953196

Tatiya-aphiradee, N., Chatuphonprasert, W., & Jarukamjorn, K. (2018). Immune response and inflammatory pathway of ulcerative colitis. *Journal of Basic and Clinical Physiology and Pharmacology*, *30*(1), 1–10. https://doi.org/10.1515/jbcpp-2018-0036

Tüysüz, N., Van Bloois, L., Van Den Brink, S., Begthel, H., Verstegen, M. M. A., Cruz, L. J., Hui, L., Van Der Laan, L. J. W., De Jonge, J., Vries, R., Braakman, E., Mastrobattista, E., Cornelissen, J. J., Clevers, H., & Ten Berge, D. (2017). Lipid-mediated Wnt protein stabilization enables serum-free culture of human organ stem cells. *Nature Communications*, *8*(1), 14578. https://doi.org/10.1038/ncomms14578

Van Der Flier, L. G., & Clevers, H. (2009). Stem Cells, Self-Renewal, and Differentiation in the Intestinal Epithelium. *Annual Review of Physiology*, *71*(1), 241–260. https://doi.org/10.1146/annurev.physiol.010908.163145

Van Der Post, S., Birchenough, G. M. H., & Held, J. M. (2021). NOX1-dependent redox signaling potentiates colonic stem cell proliferation to adapt to the intestinal microbiota by linking EGFR and TLR activation. *Cell Reports*, *35*(1), 108949. https://doi.org/10.1016/j.celrep.2021.108949

Xing, C., Liang, G., Yu, X., Zhang, A., Luo, X., Liu, Y., Tang, Z., Wu, B., Song, Z., & Lan, D. (2023). Establishment of Epithelial Inflammatory Injury Model Using Intestinal Organoid Cultures. *Stem Cells International*, *2023*, 1–13. https://doi.org/10.1155/2023/3328655

Zhao, S., Jiang, E., Chen, S., Gu, Y., Shangguan, A. J., Lv, T., Luo, L., & Yu, Z. (2016). PiggyBac transposon vectors: The tools of the human gene encoding. *Translational Lung Cancer Research*, *5*(1), 120–125. https://doi.org/10.3978/j.issn.2218-6751.2016.01.05

Zhao, Z., Chen, X., Dowbaj, A. M., Sljukic, A., Bratlie, K., Lin, L., Fong, E. L. S., Balachander, G. M., Chen, Z., Soragni, A., Huch, M., Zeng, Y. A., Wang, Q., & Yu, H. (2022).

Organoids. *Nature Reviews Methods Primers*, *2*(1), 94. https://doi.org/10.1038/s43586-022-00174-y

6. List of figures

7. List of tables